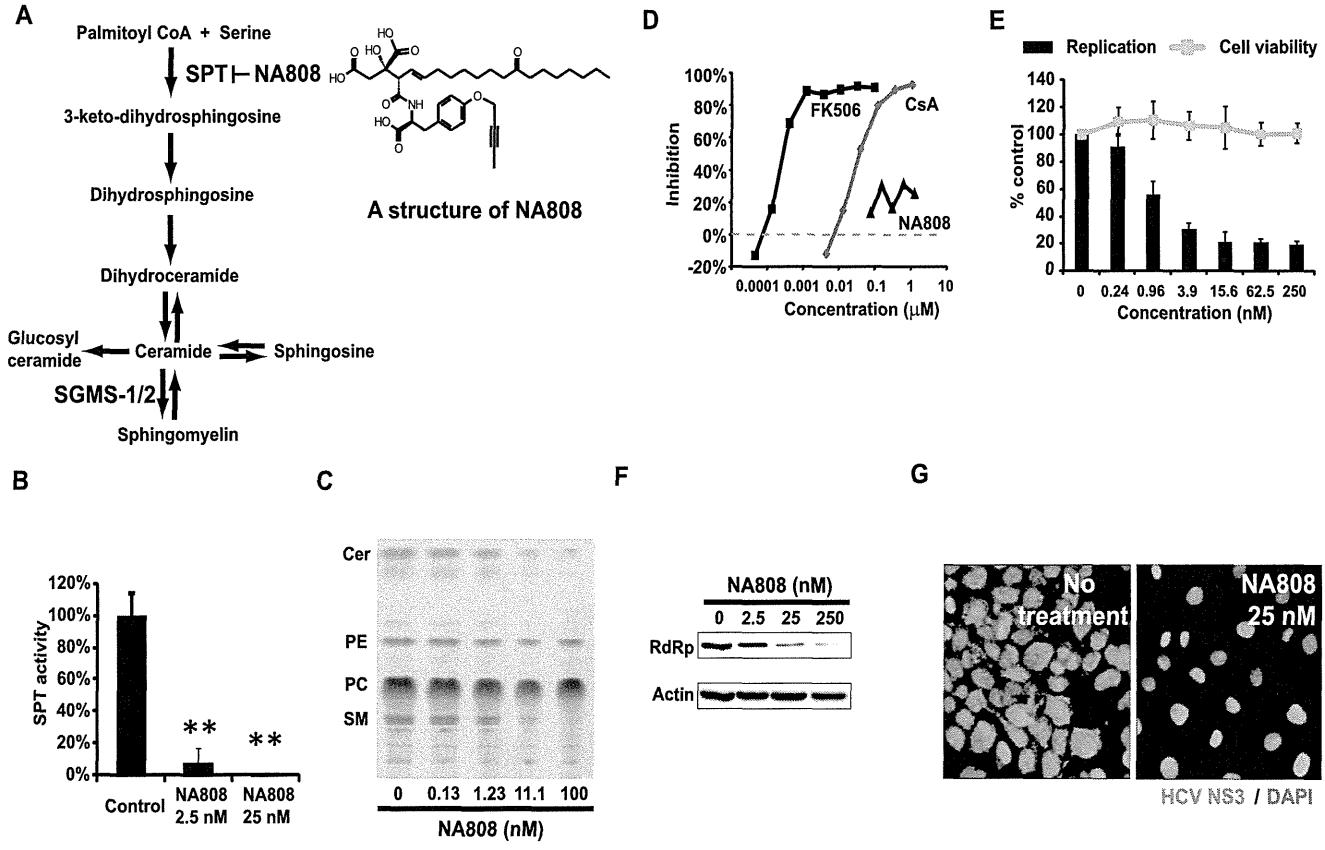

Figure 3. Characterization of the hepatotropic serine palmitoyltransferase inhibitor NA808. (**A**) Sphingolipid biosynthesis pathway and structure of NA808. (**B**) Activity of SPT in FLR3-1 cells after 72 h of NA808 treatment. $^{**}p<0.01$ compared with control. (**C**) Results of TLC showing *de novo* sphingolipid biosynthesis in the presence of NA808. Cer = ceramide, PE = phosphatidylethanolamine, PC = phosphatidylcholine, SM = sphingomyelin. (**D**) Immunosuppressive activity of NA808. Cyclosporin A (CsA) and tacrolimus (FK-506) were used as positive controls. (**E**) Effects of NA808 on HCV replication (black bars) and cell viability (gray symbols) in FLR 3-1 replicon-containing cells. Error bars indicate SDs. (**F**) Effects of NA808 on the level of the RdRp and β-actin, as assessed by Western blotting. (**G**) Effect of NA808 on the production of HCV NS3 protein (green) in FLR3-1 replicon-containing cells, as assessed by immunofluorescence analysis. Nuclear DNA was stained with DAPI (blue).
doi:10.1371/journal.ppat.1002860.g003

(**Figure 4B**). Notably, in 2 of 5 chimeric mice, serum HCV-RNA was not detectable at the end of the 21-day regimen. Consistent with this observation, the levels of both hepatic HCV-RNA and HCV core protein decreased significantly ($p<0.01$ and $p<0.05$, respectively) following NA808 treatment, these effects being dose dependent (**Figure 4C**). Immunofluorescence analysis and immunohistochemistry confirmed the reduced abundance of HCV core protein after 14 days of treatment (**Figure 4D and Figure S3**).

In genotype 2a-infected chimeric mice, NA808 decreased serum HCV-RNA by approximately 3 log units within 14 days (**Figure 4E**). NA808-treated mice displayed a corresponding reduction in hepatic HCV-RNA (**Figure 4F**). NA808 did not affect body weight or human serum albumin levels (**Figures S4A and S4B**). Furthermore, hematoxylin and eosin (H&E) staining revealed little morphological change in response to treatment with NA808. Immunofluorescence analysis also indicated that NA808 did not affect the production of human albumin (**Figure S4C**). Thus, inhibition of sphingolipid biosynthesis by an SPT inhibitor impeded HCV replication in an animal infection model, regardless of HCV genotype.

Inhibition of SPT decreases ceramide and SM levels in hepatocytes of humanized chimeric mice

We next investigated the effects of sphingolipid biosynthesis inhibition on SM and ceramide levels in hepatocytes of humanized chimeric mice. Pharmacokinetic analysis in a rat model indicated that NA808 has hepatotropic properties (**Table S1**). Consistent with this analysis, our study in chimeric mice also indicated that the NA808 concentration was much higher in the liver than in serum (**Figure S5**). Furthermore, we observed that serum SM content was not decreased by NA808 treatment (**Figure S6**), in contrast to the effects previously observed for myriocin, another SPT inhibitor [19].

In HCV-infected chimeric mouse hepatocytes, MS analysis indicated that HCV infection resulted in increased ceramide and SM levels. However, treatment of infected animals with NA808 (5 mg/kg) attenuated this increase in ceramide and SM levels in hepatocytes, and the change in SM was significant ($p<0.05$) compared to the level observed in HCV-infected chimeric mice with no treatment. This effect of NA808 on ceramide and SM levels was dose-dependent (**Figures 5A and 5B**). We also found that SM levels and hepatic HCV-RNA were correlated (**Figure 5C**).

Interestingly, treatment with NA808 effectively decreased two specific SM and ceramide molecular species (*d*18:1-22:0 and *d*18:1-24:0), slightly decreased one other species (*d*18:1-24:1), and hardly decreased another (*d*18:1-16:0). Further, we found that among SM and ceramide molecular species, *d*18:1-16:0 did not change (**Figures 5D and 5E**). These results indicate that the

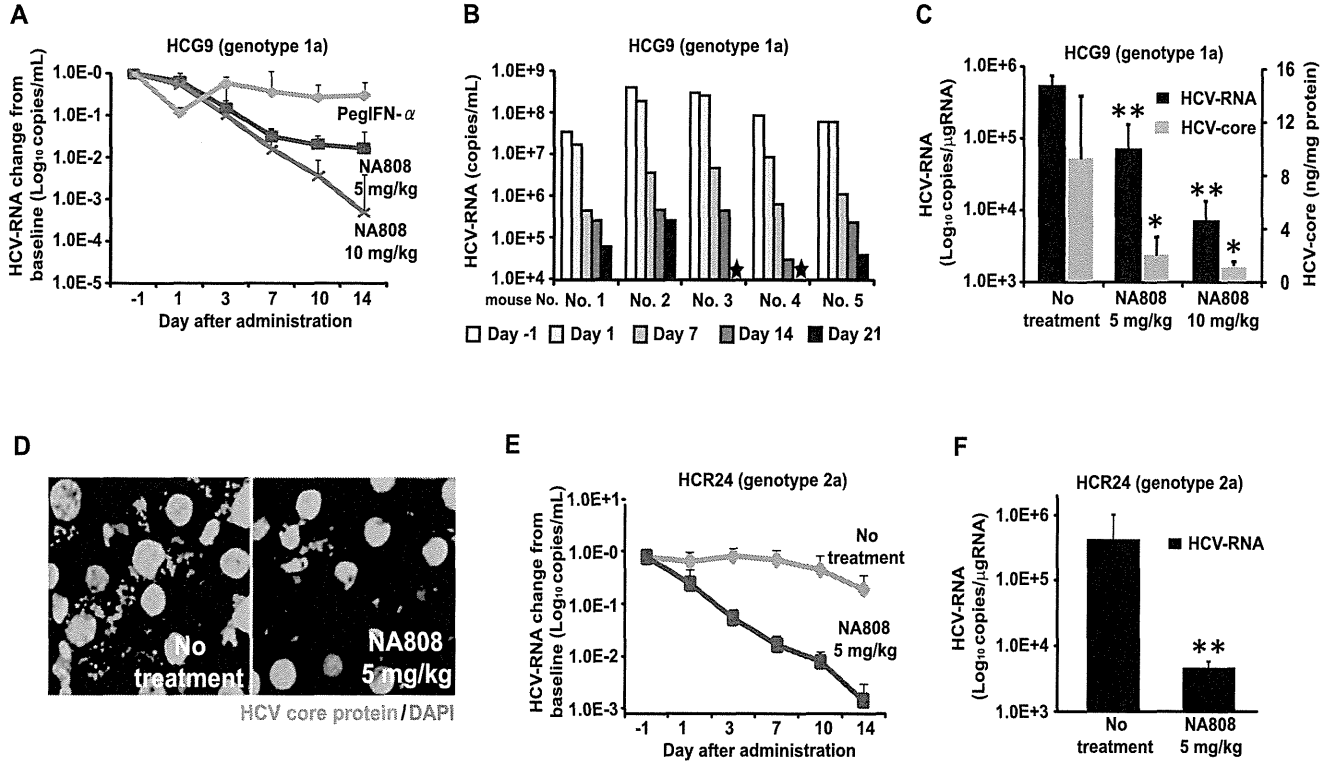

Figure 4. Inhibition of sphingolipid biosynthesis with hepatotropic serine palmitoyltransferase (SPT) inhibitor NA808 exerts anti-HCV effect. (**A**) Serum HCV-RNA levels in response to treatment with NA808 (blue, 5 mg/kg/day, purple, 10 mg/kg/day, n = 6 each), or PegIFN-α (pink, 30 μg/kg twice weekly, n = 4). (**B**) Effect of NA808 (5 mg/kg/day) on serum HCV-RNA levels. A star indicates that HCV-RNA was not detected. (**C**) Levels of liver HCV-RNA (black) and HCV core protein (gray) after the 14-day treatment. *$p<0.05$ and **$p<0.01$ compared with no treatment. (**D**) Histological analysis using immunofluorescent labeling of HCV core protein (green) and fluorescent staining of nuclei (blue). (**E**) Serum HCV-RNA levels in response to no treatment (pink, n = 3) or NA808 treatment (blue, 5 mg/kg/day, n = 4). (**F**) Liver HCV-RNA levels in genotype 2a-infected mice after the 14-day treatment. *$p<0.05$ and **$p<0.01$ compared with no treatment. In all cases, error bars indicate SDs.
doi:10.1371/journal.ppat.1002860.g004

effects of sphingolipid biosynthesis inhibition varied among the molecular species.

Considering these results, we found a discrepancy in SM molecular species which were considered to be important for HCV replication. To elucidate the relationship between SM molecular species and HCV replication, we attempted to identify endogenous SM molecular species comprising the DRM fraction and to evaluate the effects of HCV infection and inhibition of sphingolipid biosynthesis on SM levels of the DRM.

Relationship between endogenous SM molecular species constituting the DRM and HCV replication

We previously reported that SM interacts with RdRp, allowing it to localize to the DRM fraction where HCV replicates and activates RdRp [7,8], and that suppression of SM biosynthesis disrupts the association between RdRp and SM in the DRM fraction, resulting in suppression of HCV replication [7,8]. In the present study, treatment with NA808 decreased SM levels in the DRM fraction; the decreased presence of SM correlated with decreased RdRp abundance, but the same effect was not seen for HCV nonstructural protein 3 (**Figures S7A–C**). Given these results, we investigated whether HCV replication was induced by elevated SM levels. Specifically, we compared SM levels in the DRM fraction between HCV-infected hepatocytes and uninfected hepatocytes. MS analysis showed that HCV increased SM levels in the DRM fraction more remarkably than in whole cells (**Figure 6A**). Next, we identified SM molecular species composing the DRM fraction and found that the composition ratio of SM molecular species was distinct between whole cells and DRM fractions in both HCV-infected and uninfected hepatocytes (**Figure 6B and Figure S8**). The DRM was composed primarily (69%) of *d*18:1-16:0, followed (in decreasing order) by *d*18:1-24:0, *d*18:1-22:0, and *d*18:1-24:1; the abundance of all SM molecular species increased upon HCV infection (**Figure 6C**). Further, NA808 treatment decreased all SM molecular species in the DRM fraction. Consistently, NS3 protease inhibitor decreased all SM molecular species in the DRM fraction of subgenomic replicon cells (**Figure S9**).

To address the association between RdRp and the endogenous SM molecular species composing the DRM, we used high-performance liquid chromatography (HPLC) to separate each SM molecular species from bulk SM derived from bovine milk and brain. We evaluated the relationship between RdRp and these endogenous SM molecular species using *in vitro* analysis. Enzyme-linked immunosorbent assay (ELISA) indicated that these endogenous SM molecular species bound to RdRp more readily than the bulk SM derived from milk as a positive control (**Figure 6D**). Further, *in vitro* HCV transcription analysis showed that three SM species (*d*18:1-16:0, *d*18:1-22:0, and *d*18:1-24:1) increased *in vitro* RdRp activation by approximately 5-fold, whereas the *d*18:1-24:0 species increased activation by 2-fold (**Figure 6E**). In a previous study, the soluble RdRp without its C-terminal hydrophobic 21-amino-acid sequence was used in *in vitro* analysis [8], and whether the relationship between RdRp and SM proved in this analysis

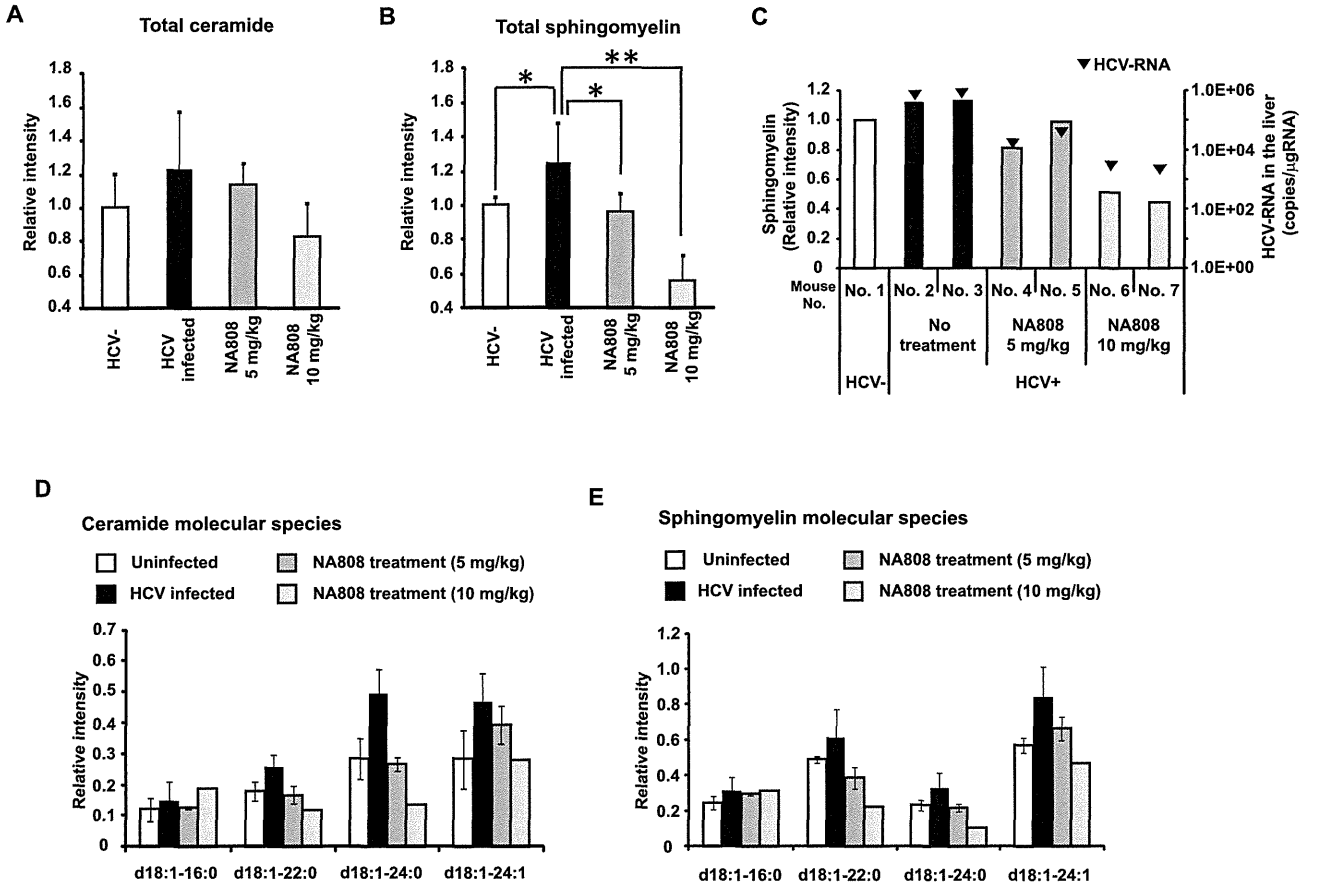

Figure 5. Effects of NA808 treatment on sphingomyelin (SM) and ceramide (total and individual molecular species). (**A, B**) Relative ratio of total ceramide (**A**) and SM (**B**) in uninfected mice (white, n = 4), HCV genotype 1a-infected mice (black, n = 5), and HCV-infected mice treated with NA808 for 14 days (dark gray, 5 mg/kg, n = 4; light gray, 10 mg/kg, n = 3). *$p<0.05$ and **$p<0.01$ compared with HCV-infected mice. (**C**) SM levels (bars) and HCV RNA levels (black arrowhead) in the livers of mice treated for 14 days with NA808 (5 or 10 mg/kg/day) and untreated chimeric mice. (**D, E**) Relative intensities of individual ceramide molecular species (**D**) and individual SM molecular species (**E**) in uninfected mice (white, n = 3), HCV-infected mice (black, n = 3), and HCV-infected mice treated with NA808 for 14 days (dark gray, 5 mg/kg, n = 2; light gray, 10 mg/kg, n = 1). In all cases, error bars indicate SDs.
doi:10.1371/journal.ppat.1002860.g005

reflected the state in the membranous replication complex remains to be elucidated. Therefore, we attempted to examine the effect of endogenous SM molecular species on HCV replicase activity *in vivo* using digitonin-permeabilized semi-intact replicon cells, which permit monitoring of the function of the active HCV replication complex (**Figure 6F**) [20]. This *in vivo* analysis also enabled us to deliver the extrinsically added SM molecular species directly to the cytosol. This RNA replication assay indicated that the endogenous SM molecular species (*d*18:1-16:0 and *d*18:1-24:0) enhanced HCV-RNA replication, these species being consistent with the two SM molecular species that primarily constitute the DRM and are decreased significantly by NA808 treatment (**Figures 6G and 6H**). These results suggest that HCV infection modifies the levels of specific endogenous SM molecular species, which in turn enhance HCV-RNA replication by interacting with RdRp.

Discussion

In this study, we showed that HCV alters sphingolipid metabolism, resulting in a better environment for viral replication. Specifically, HCV increased SM content in the DRM fraction; this step is essential for viral replication since SM is a key component of the membranous replication complex and interacts with RdRp. Employing MS analysis, we identified endogenous SM molecular species (located in the DRM fraction) that increased upon HCV infection, and demonstrated that these endogenous SM molecular species interact directly with RdRp, enhancing HCV replication. Thus, we concluded that HCV modulates sphingolipid metabolism to promote viral replication.

We found that the expression levels of SGMS1/2 and the content of SM and ceramide in HCV-infected humanized chimeric mouse livers was increased (Figure 1). Our measurement revealed that chronic HCV infection promoted sphingolipid biosynthesis. HCV is known to induce cellular stress [21,22]. A variety of cell stressors increase intracellular ceramide content during the execution phase of apoptosis [23,24], indicating that ceramide is a proapoptotic lipid mediator. Furthermore, activation of ceramide-metabolizing enzymes such as glucosylceramide synthase and SM synthase can attenuate apoptosis by decreasing the intracellular ceramide content [25,26]. We found that HCV infection correlated with increased mRNA levels of the genes that encode human SM synthases (*SGMS1/2*) and glucosylceramide synthase (*UGCG*) (data not shown). Thus, the increase in ceramide levels observed in our study was likely to activate enzymes that transfer ceramide to other sphingolipids. On the other hand, Diamond et al. reported on lipidomic profiling performed over the

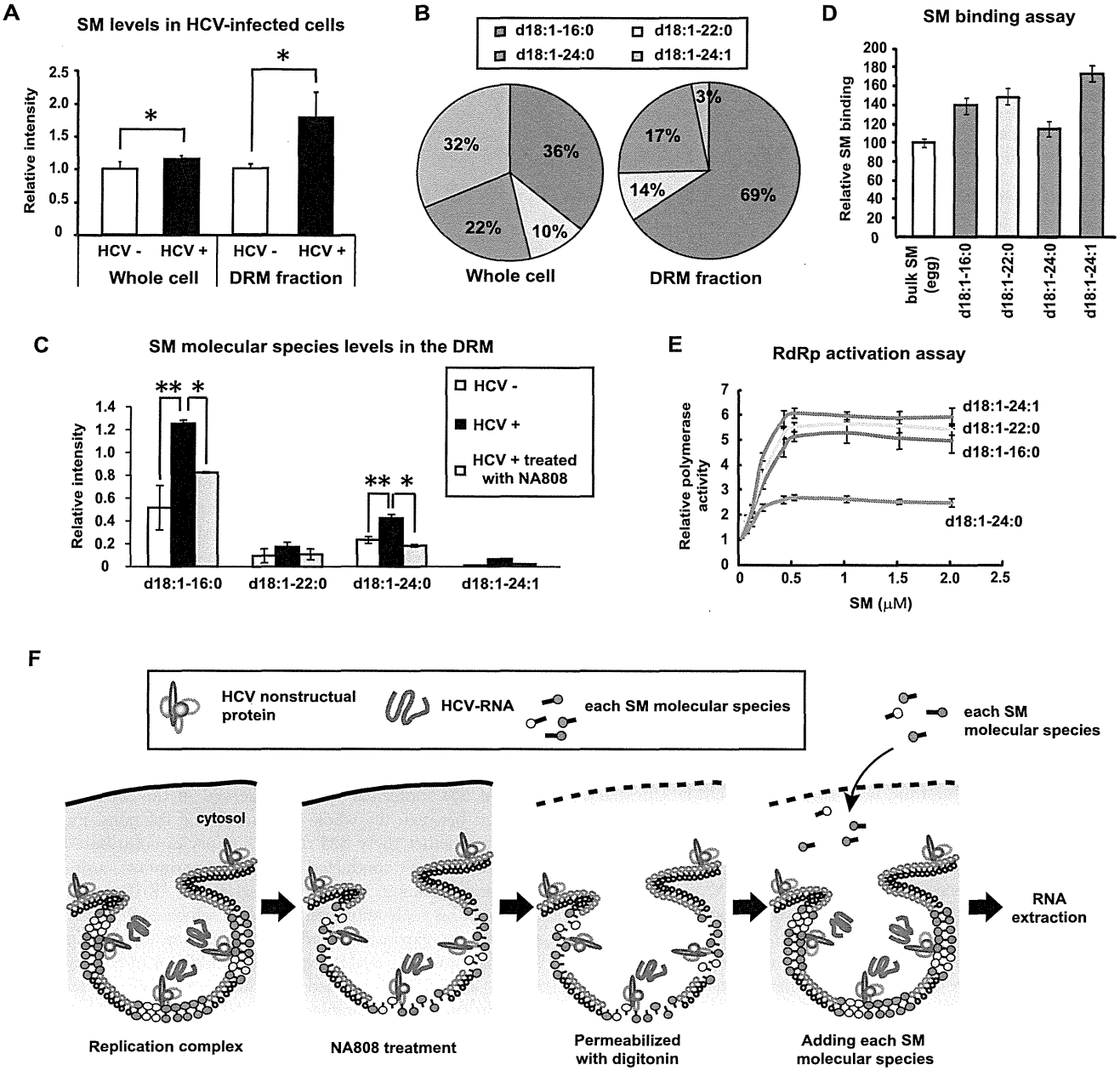
A
SM levels in HCV-infected cells
Relative intensity
HCV - HCV + HCV - HCV +
Whole cell
DRM fraction
B
d18:1-16:0
d18:1-22:0
d18:1-24:0
d18:1-24:1
32%
36%
22%
10%
Whole cell
17%
3%
14%
69%
DRM fraction
D
SM binding assay
Relative SM binding
bulk SM (egg)
d18:1-16:0
d18:1-22:0
d18:1-24:0
d18:1-24:1
C
SM molecular species levels in the DRM
Relative intensity
HCV -
HCV +
HCV + treated with NA808
d18:1-16:0
d18:1-22:0
d18:1-24:0
d18:1-24:1
E
RdRp activation assay
Relative polymerase activity
d18:1-24:1
d18:1-22:0
d18:1-16:0
d18:1-24:0
SM (μM)
F
HCV nonstructual protein
HCV-RNA
each SM molecular species
each SM molecular species
cytosol
RNA extraction
Replication complex
NA808 treatment
Permeabilized with digitonin
Adding each SM molecular species
G
HCV-RNA replication assay in permeabilized replicon cells
HCV-RNA (% of control)
(μM)
16:0 SM
22:0 SM
24:0 SM
24:1 SM
H
HCV-RNA replication assay in permeabilized replicon cells with NA808 treatment
p = 0.085
p = 0.21
p = 0.034
p = 0.27
HCV-RNA (% of control)
NA808 treatment (-)
(μM)
16:0 SM
22:0 SM
24:0 SM
24:1 SM

Figure 6. Specific sphingomyelin molecular species upregulated by HCV promote HCV replication on the detergent-resistant membrane fraction. (**A**) Comparison of the relative amounts of SM, as measured by MS analysis, in whole cells and the DRM fraction of mock-infected (HuH-7 K4 cells) (white, n = 6; whole cells, n = 3; DRM fraction) and HCV (JFH-1)-infected cells (JFH/K4 cells) (black, n = 6; whole cells, n = 3; DRM fraction). (**B**) Composition ratio of SM molecular species in whole cells and DRM fraction of HCV-infected cells. (**C**) Relative intensities of each SM molecular species in the DRM fraction of mock-infected cells (white, n = 2) and HCV-producing cells without (black, n = 2) or with NA808 treatment (gray, n = 2). (**D**) Results of the ELISA SM binding assay (n = 3 each). (**E**) Average activation kinetics of each SM molecular species on HCR6 (genotype 1b) RdRp (n = 3 each). (**F**) Scheme of HCV-RNA replicase assay using digitonin-permeabilized cells. (**G, H**) Effect of each SM molecular species on HCV-RNA in digitonin-permeabilized replicon cells treated without (G) or with 10 nM NA808 (H) (n = 3 each). In all cases, error bars indicate SDs. $*p<0.05$ and $**p<0.01$.
doi:10.1371/journal.ppat.1002860.g006

time course of acute HCV infection in cultured Huh-7.5 cells and observed that specific SM molecular species were decreased 72 h after HCV infection [27]. Given that their study focused on acute HCV infection, the reason for this discrepancy may be due to the severity of infection, suggesting that the influence of HCV infection on sphingolipid metabolism differs between acute and chronic infections. We also demonstrated that HCV infection correlates with increased abundance of specific SM and ceramide molecular species, with the profiles of individual lipids differing for infection by HCG9 (genotype 1a) and HCR24 (genotype 2a). The precise mechanism and meaning of these differences remain to be elucidated.

Our results indicated that SGMS1 expression had a correlation with HCV replication. This indicates that SM synthesized by SGMS1 contributes to HCV replication. A previous report revealed that in cultured cell lines, SGMS1 localizes in Golgi apparatus while SGMS2 localizes in the plasma membrane [28]. Thus, the results of this previous report suggest that SMs synthesized by SGMS1 can be easily incorporated into membranous replication complexes. As for SGMS2, we found that HCV infection significantly increased the expression of SGMS2, although the relationship between SGMS2 and HCV replication was hardly seen in this study. The relationship between SGMS2 and HCV propagation, thus, is an issue that should be elucidated in future studies.

We also demonstrated in this study that reduction of SM molecular species by NA808, a hepatotropic SPT inhibitor with little immunosuppressive activity, inhibits HCV replication in humanized chimeric mice regardless of viral genotype (Figure 4). Notably, treatment with NA808 (5 mg/kg) restored SM and ceramide levels in the liver to the levels observed in uninfected chimeric mice (Figure 5). Apparently, a slight reduction in SM had a significant influence on HCV, indicating that SM plays an important role in the HCV life cycle. SM is required for many viral processes in host-pathogen interactions [29–31]. For instance, viral envelopes of human immunodeficiency virus type 1 (HIV-1) and herpes simplex virus (HSV) are enriched with SM, which is necessary for efficient virus infectivity [32,33]. With regard to HCV, in addition to efficient virus infectivity [34], SM is present in the raft domain, which serves as a site of virus replication, together with other sphingolipids and cholesterol [6]. Moreover, SM is a component of VLDL whose assembly component and pathway is required for HCV morphogenesis and secretion [34,35]. The above-mentioned observations suggest that SM plays a multifaceted role in the HCV life cycle; therefore, SM is likely to be a good therapeutic target.

HCV is thought to replicate in a specialized compartment characterized as a DRM (designated as the membranous replication complex) [6]. SM, cholesterol, and phosphatidylinositol (PI) are thought to be the lipids that make up the membranous replication complex. With regard to PI, several siRNA screening have recently identified type III phosphatidylinositol 4-kinases (PI4K) as crucial host factors for HCV replication [36–39]. In HCV replicon containing cells, PI4P distribution is altered and enriched in the membranous replication complex by PI4KIIIα synthesis. Although the ability of PI to influence membrane bending and regulate intracellular processes (e.g. vesicle fusion, budding, and sorting) has been reported, the role of PI4P in the formation of the membranous replication complex remains to be elucidated. SM and cholesterol organize the solid membrane characterized as the DRM, where HCV replicates [6]. In fact, we and other groups demonstrated that reduction of SM and cholesterol suppressed HCV replication [7,9,12,40]. We performed the immunofluorescent analysis using lysenin. However, lysenin did not co-localize with NS4B protein. To date, it has been reported that lysenin-binding to SM is increased in the form of SM clusters, and that glycosphingolipids hinder lysein-binding to SM [41] Lipid rafts form of HCV replication complex do not have the characters of lysenin-binding to SM.

Further, the role of SM is not only to act as a constituent of the membranous replication complex, but also to bind and activate RdRp [7,8]. In this study, to gain further insight into the HCV membranous replication complex, we attempted to analyze which SM molecular species comprise the membranous replication complex, given that the diversity of molecular species is believed to be responsible for the physiochemical properties of the biomembrane [42] (Figure 6). We found that the composition ratio of SM molecular species observed in this study was quite different between the whole cell and DRM fractions. Further, to identify whether these SM molecular species contribute to HCV replication, we conducted rescue experiments using HCV replicon-containing cells (carrying intact RdRp and active membranous replication complexes) in which each SM molecular species was extrinsically added to replicon cells treated with NA808. However, in this experiment, addition of SM caused cell death. Therefore, we used digitonin-permeabilized semi-intact replicon cells, which enabled us to deliver the extrinsically added SM molecular species directly to the cytosol without catalytic effect and permitted monitoring of intact RdRp and replication complexes. We demonstrated that the specific endogenous SM molecular species (*d*18:1-16:0 and *d*18:1-24:0) enhance HCV-RNA replication, these species being consistent with the two SM molecular species which mainly constitute the DRM. Collectively, these results suggest that the HCV replication complex characterized as DRM is the specialized compartment that is composed of SM molecular species. These findings will provide new insights into the formation of the HCV replication complex and the involvement of host lipids in the HCV life cycle.

Materials and Methods

Ethics statement

This study was carried out in strict accordance with both the Guidelines for Animal Experimentation of the Japanese Association for Laboratory Animal Science and the recommendations in the Guide for the Care and Use of Laboratory Animals of the National Institutes of Health. All protocols were approved by the ethics committee of Tokyo Metropolitan Institute of Medical

Science. The patient with HCV infection who provided the serum samples gave written informed consent before blood collection.

Cells

The HCV subgenomic replicon cells FLR3-1 (genotype 1b, Con-1) was cultured at 37°C in Dulbecco's modified Eagle's medium GlutaMax-I (Invitrogen, Carlsbad, CA, USA) supplemented with 10% fetal bovine serum (FBS) and 0.5 mg/mL G418. HuH-7 K4 cells (cured of HCV by IFN treatment) and the JFH/K4 cells persistently infected with the HCV JFH-1 strain were maintained in DMEM containing 10% FCS and 0.1 mg/mL penicillin and streptomycin sulfate. MH-14 cells were grown in Dulbecco's modified Eagle's medium supplemented with 10% fetal bovine serum, 100 U/mL nonessential amino acids, 0.1 mg/mL penicillin and streptomycin sulfate, and 0.5 mg/mL G418.

siRNA assay

siCONTROL, siSGMS1, and siSGMS2 were purchased from Dharmacon RNA Technologies (Lafayette, CO, USA). The siCONTROL Non-Targeting siRNA #3 was used as the negative control siRNA. We used siRNAs against the HCV genome (siE-R7) [16]. The chemically synthesized siRNAs were transfected into cells using Lipofectamine RNAiMAX (Invitrogen) and Opti-MEM (Invitrogen) by reverse-transfection. Cells were characterized at 96 h after transfection.

Serine palmitoyltransferase activity

We assessed SPT activity in the liver as previously described, with minor modifications [43]. Briefly, frozen cells were homogenized in HEPES buffer (10 mM HEPES, 2 mM sucrose monolaurate, and 0.25 M sucrose, pH 7.4), and homogenates were centrifuged at 10,000×*g* for 20 min. From the resulting supernatant, samples containing 200 μg protein were assayed for SPT activity using [^{14}C]-serine and palmitoyl-CoA (Sigma-Aldrich, St. Louis, MO, USA) as substrates.

Proliferation assay

Human peripheral blood cells (AllCells, Emeryville, CA, USA) were plated onto 96-well plates and treated with phytohemagglutinin with or without immunosuppressant reagents. After 2 days of stimulation, [^{3}H]-thymidine-containing growth medium was added, and the cultures were incubated for another 18 h. T-cell proliferation was assessed by comparing the level of thymidine incorporation to that in the stimulated control.

Anti-hepatitis C virus assay in Huh-7 cells harboring subgenomic replicons

Replication was determined after 72 h with a Bright-Glo luciferase assay kit (Promega, Madison, WI, USA). The viability of replicon cells was determined using a cell counting kit (Dojindo, Kumamoto, Japan) according to the manufacturer's instructions.

Western blot analysis

Cells were resuspended in lysis buffer (10 mM Tris, pH 7.4 containing 1% SDS, 0.5% Nonidet P-40, 150 mM NaCl, 0.5 mM EDTA, and 1 mM dithiothreitol). Ten micrograms of the resulting protein sample were electrophoresed on a 10% sodium dodecyl sulfate-polyacrylamide gel and subsequently transferred to a polyvinylidene difluoride membrane (Immobilon-P; Millipore, Billerica, MA, USA). HCV nonstructural protein 3 (NS3) and nonstructural 5B polymerase (RdRp) were detected with rabbit anti-NS3 polyclonal antibody (R212) and mouse anti-RdRp monoclonal antibody (5B-14) prepared in our laboratory. β-Actin was detected with anti-β-actin monoclonal antibody (Sigma-Aldrich).

Immunofluorescent staining of hepatitis C virus replicon cells

After treatment with 25 nM NA808 for 96 h, FLR3-1 cells were probed with anti-NS3 polyclonal antibody (R212; the primary antibody). Next, an anti-rabbit IgG-Alexa 488 conjugate (Invitrogen) was applied as the secondary antibody.

Thin-layer chromatography analysis

Thin-layer chromatography (TLC) analysis was performed as described previously [9]. Briefly, cells were incubated with [^{14}C]-serine in Opti-MEM (Invitrogen). Cells extracts were obtained using the Bligh & Dyer method [44] and were spotted onto Silica Gel 60 TLC plates (Merck, Darmstadt, Germany) for separation. Radioactive spots were detected using a BAS 2000 system (Fuji Film, Kanagawa, Japan).

Membrane flotation assay

Cells were lysed in TNE buffer (25 mM Tris-HCl, 150 mM NaCl, 1 mM EDTA) and passed 20 times through a 25-gauge needle. Nuclei and unbroken cells were removed by centrifugation at 1,000×*g* for 5 min. After ensuring that the amount of total protein was equivalent across all samples, cell lysates were treated with 1% Triton on ice for 30 min and then subjected to a sucrose gradient (10%, 30%, and 40%). The sucrose gradient was centrifuged at 247,220×*g* in a Beckman SW41 Ti rotor (Beckman Coulter Inc., Brea, CA, USA) for 14 h at 4°C. Fractions (1 mL) were collected from the top of the gradient.

Infection of mice with hepatitis C virus genotypes 1a and 2a

Chimeric mice infected with HCV were prepared as previously described [45]. Briefly, approximately 40 days after the transplantation procedure, mice were intravenously injected with 5×10^5 copies/mouse of HCG9 (genotype 1a) or HCR24 (genotype 2a) that had been collected from patient serum.

Quantification of HCV RNA by real-time polymerase chain reaction

Total RNA was purified from 1 μL of chimeric mouse serum using SepaGene RV-R (Sanko Junyaku Co. Ltd., Tokyo, Japan) and from liver tissue using Isogene (Nippon Gene Co. Ltd., Tokyo, Japan). HCV RNA was quantified by quantitative real-time polymerase chain reaction (PCR) using previously reported techniques [9]. For serum, this technique has a lower limit of detection of 4000 copies/mL. Therefore, samples in which HCV RNA was undetectable were assigned this minimum value.

Quantification of HCV core protein by ELISA

Liver specimens were homogenized in TNE buffer. Aliquots of 5 μg of total protein were assayed for core protein levels with an Ortho HCV core protein ELISA kit (Eiken Chemical, Tokyo, Japan).

Indirect immunofluorescence analysis

The primary antibody for immunofluorescence analysis of liver sections was anti-HCV core protein monoclonal antibody (5E3) [46]. Monoclonal antibody labeling was followed by staining with anti-mouse IgG Alexa-488. The nuclei were stained using 4′,6-diamidino-2-phenylindole (DAPI).

Gene expression analysis

To measure mRNA levels, total RNA samples were extracted from the mouse livers and cDNA was synthesized using a High-Capacity cDNA Reverse Transcription Kit (Applied Biosystems, Foster City, CA, USA). The cDNA solution was assessed by quantitative PCR performed with TaqMan Gene Expression Assays (Applied Biosystems) and an ABI 7700 Sequence Detection System (Applied Biosystems).

Quantification of SM and ceramide in liver

We quantified liver SM and ceramide levels using a mass spectrometer (MS). Electrospray ionization (ESI)-MS analysis was performed using a 4000Q TRAP quadrupole-linear ion trap hybrid MS (AB SCIEX, Foster City, CA, USA) with an UltiMate 3000 nano/cap/micro-liquid chromatography system (Dionex Corporation, Sunnyvale, CA, USA) combined with an HTS PAL autosampler (CTC Analytics AG, Zwingen, Switzerland). The total lipid fractions expected to contain SM and ceramide, were subjected directly to flow injection and were selectively analyzed by neutral loss scanning of 60 Da (HCO_2+CH_3) from SM $[M+HCOO]^-$ in the negative ion mode, and multiple-reaction monitoring using a combination of ceramide $[Cer-H_2O+H]^+$ and the product (long-chain base) $[LCB-H_2O+H]^+$ in the positive ion mode [47,48]. The mobile phase composition was acetonitrile:methanol:water at 6:7:2 (0.1% ammonium formate, pH 6.8) and a flow rate of 10 μL/min. The typical injection volume was 3 μL of total lipids, normalized by protein content.

LC/ESI-MS analysis was performed using quadrupole/time of flight (Q-TOF) micro with an ACQUITY UPLC system (Waters Corporation, Milford, MA, USA) in the negative ion mode and an Agilent 6230 with an Agilent 1290 Infinity LC system (Agilent Technologies, Inc., Loveland, CO, USA) in the positive ion mode. Reversed-phase LC separation was achieved using an ACQUITY UPLC BEH column (150 mm×1.0 mm i.d., Waters Corporation) at 45°C. The mobile phase was acetonitrile:methanol:water at 19:19:2 (0.1% formic acid+0.028% ammonia) (A) and isopropanol (0.1% formic acid+0.028% ammonia) (B), and the composition was produced by mixing these solvents. The gradient consisted of holding A:B at 90:10 for 7.5 min, then linearly converting to A:B at 70:30 for 32.5 min, and then linearly converting to A:B at 40:60 for 50 min. The detailed procedure for LC/ESI-MS was described previously [49,50].

Separation of SM molecular species by HPLC

Bovine milk or brain SM (Avanti Polar Lipids. Inc., Alabaster, AL, USA) was dissolved in chloroform:methanol (2:1), then separated according to molecular species by reversed-phase HPLC. The *d*18:1-16:0, 22:0, and 24:0 molecular species of SM were isolated from bovine milk SM, while the *d*18:1-24:0 and 24:1 molecular species were isolated from brain SM. Bovine milk and brain SM were then separated on Senshu PAK ODS (C18) columns (Senshu Scientific Co., Ltd., Tokyo, Japan) using methanol as the eluting solvent at a flow rate of 1 mL/min. The fatty acid compositions of the purified fractions were analyzed by LC/ESI-MS. The amount of SM in each fraction was quantified using an SM assay kit (Cayman Chemical, Ann Arbor, MI, USA). We confirmed that the purity of each molecular species was approximately 90% without *d*18:1-24:1 (about 70%) (data not shown).

In vitro HCV transcription

In vitro HCV transcription was performed as previously described [8].

SM binding assay using ELISA

An SM binding assay was performed as previously described [8] using rabbit anti-HCV RdRp sera (1:5000) and an HRP-conjugated anti-rabbit IgG antibody (1:5000). Optical density at 450 nm (OD_{450}) was measured on a Spectra Max 190 spectrophotometer (Molecular Devices, Sunnyvale, CA, USA) using the TMB Liquid Substrate System (Sigma).

RNA replication assays in permeabilized replicon cells

The analysis using digitonin-permeabilized replicon cells was performed as previously described [20] with minor modifications. Briefly, MH-14 cells of about 80% confluency were pre-cultured for 2 h in complete Dulbecco's modified Eagle's medium containing 5 μg/mL actinomycin D (Nacalai Tesque, Kyoto, Japan), then washed with cold buffer B (20 mM HEPES-KOH (pH 7.7 at 27°C), 110 mM potassium acetate, 2 mM magnesium acetate, 1 mM EGTA, and 2 mM dithiothreitol). The cells were permeabilized by incubation in buffer B containing 50 μg/mL digitonin for 5 min at 27°C, and the reaction was stopped by washing twice with cold buffer B. The permeabilized cells were then incubated for 4 h at 27°C in the reaction mixture with or without each lipid. The reaction mixture consisted of 2 mM manganese(II) chloride, 1 mg/mL acetylated bovine serum albumin (Nacalai Tesque), 5 mM phosphocreatine (Sigma), 20 units/mL creatine phosphokinase (Sigma), 50 μg/mL actinomycin D, and 500 μM each of ATP, CTP, GTP, and UTP (Roche Diagnostics, Basel, Switzerland) in buffer B (pH 7.7). Total RNA was purified by the acid guanidinium-phenol-chloroform method. In this assay, considering that the estimated SM content in human hepatocytes is 3–4 nmol/mg protein, as demonstrated by MS analysis (**Figure S10**), the amount of SM we added in the replicase assay was 0.3–1 μM. (i.e. 0.03–0.3 nmol/0.3 mL/0.1 mg protein/12 well; the reaction volume in the replicase assay was 0.3 mL/12 wells and each well of the 12 well cell culture plates contained approximately 0.1 mg protein.)

Statistical analysis

Statistical analysis was performed using the Student's *t*-test equipped with Excel 2008 (Microsoft, Redmond, WA, USA). To measure the strength of the association, Pearson correlation coefficient was calculated using Excel 2008. A p-value<0.05 was considered statistically significant.

Supporting Information

Figure S1 Impacts of HBV infection on expression of sphingomyelin (SM) biosynthesis genes. mRNA expression of *SGMS1* and *SGMS2* genes (encoding SM synthases 1 and 2, respectively) in uninfected (white) and infected (black) chimeric mice (n = 5 per group).
(JPG)

Figure S2 Effect of HCV infection in cultured cells. Comparison of the relative amounts of SM, as measured by MS analysis, in mock-infected (HuH-7 K4 cells) (white) and HCV (JFH-1)-infected cells (JFH/K4 cells) (black) (n = 1 per group).
(JPG)

Figure S3 The expression of HCV core protein in HCV-infected chimeric mice. Histological analysis using immunohistochemical labeling of HCV core protein.
(JPG)

Figure S4 Effects of NA808 on HCV-infected chimeric mice. (**A**) Average body weight of mice during treatment. (**B**) Average human albumin concentrations in the sera of mice during

treatment. (**C**) Histological analysis using H&E staining and immunofluorescent labeling of human albumin (red). In all cases, error bars indicate SDs.
(JPG)

Figure S5 Concentrations of NA808 in chimeric mice receiving NA808 treatment. Concentration of NA808 in the liver (gray) and serum (black) of chimeric mice treated with 5 mg/kg or 10 mg/kg NA808. Stars indicate that NA808 level was not detected.
(JPG)

Figure S6 Sphingomyelin (SM) levels in the serum of chimeric mice receiving NA808 treatment. SM levels in the serum of chimeric mice (n = 3 per group) that were uninfected (HCV−), or infected (HCV+) but untreated or treated with 5 or 10 mg/kg NA808. Error bars indicate SDs.
(JPG)

Figure S7 Effects of NA808 on associations between the HCV nonstructural 5B polymerase (RdRp) and sphingomyelin (SM). (**A**) Comparison of SDS-PAGE and TLC results for replicon cells receiving no treatment (Control) or NA808 treatment (NA808). NA808 dosage was 2.5 nM (for TLC) or 25 nM (for SDS-PAGE). (**B**) Relative band intensities of RdRp and NS3 in detergent-resistant membrane (DRM) fractions from cells receiving no treatment (Control) or 25 nM NA808 treatment (NA808). (**C**) Relative band intensities of SM in DRM fractions from cells receiving no treatment (Control) or 2.5 nM NA808 treatment (NA808).
(JPG)

Figure S8 Composition ratio of SM molecular species in whole cells and DRM fraction of uninfected cells.
(JPG)

Figure S9 Effect of NS3 protease inhibitor on SM molecular species in the DRM fractions of subgenomic replicon cells. (A) Effect of NS3 protease inhibitor (VX950) on HCV replication (dark grey bars) and cell viability (light grey bars) in FLR3-1 replicon-containing cells. Error bars indicate SD. (B) Effect of NS3 protease inhibitor (VX950; 3 μM) on SM molecular species of DRM fractions of FLR 3-1 replicon-containing cells. Error bars indicate SDs.
(JPG)

Figure S10 The estimated SM content in human hepatocytes. Left bar (white) indicates the intensity of SM internal standard (SM d18:0-12:0; 1 nmol) by mass spectrometer. Right bar indicates the intensity of 1 mg protein of human hepatocyte (HuH-7 K4).
(JPG)

Table S1 Distribution of radioactivity in tissues after a single intravenous administration of [^{14}C] NA808 at 2 mg/kg to non-fasting male rats.
(PDF)

Table S2 Treatment administration for HCV-infected chimeric mice. Administration of reagents was started at day 0. The amount of NA808 was adjusted according to the body weight of the mice. Dose began at 5 mg/kg or 10 mg/kg and was reduced by half at each 10% reduction in body weight (half circle). At 20% reduction, administration was discontinued. Open circle indicates each manipulation was performed as required.
(PDF)

Text S1 Materials and methods for supporting information. Methods for "Infection of chimeric mice with hepatitis B virus", "Quantification of human albumin", "Histological staining and indirect immunofluorescence analysis", and "Quantification of sphingomyelin (SM) in serum" are described.
(DOCX)

Acknowledgments

We are very grateful to Dr. Makoto Hijikata of the Department of Viral Oncology, Institute for Virus Research, Kyoto University for his technical support. We thank Isao Maruyama and Hiroshi Yokomichi of PhoenixBio Co., Ltd. for maintenance of and technical assistance with the chimeric mice.

Author Contributions

Conceived and designed the experiments: M. Kohara. Wrote the paper: Y. Hirata. Y. Hirata performed the experiment of chimeric mice and HCV-infected cells. K. Ikeda, M. Ohta, T. Soga, and R. Taguchi performed lipid analysis by MS spectrometry. M. Sudoh, A. Katsume, and Y. Aoki evaluated the antiviral effects of NA808, K. Okano and K. Ozeki examined the tissue distribution of NA808. K. Kawasaki and T. Tsukuda synthesized derivatives from natural compounds. Y. Tokunaga, Y. Tobita, T. Umehara, and S. Sekiguchi performed some experiments on the chimeric mice. L. Weng and T. Toyoda conducted the experiments on the interaction between RdRp and SM. M. Kohara and Y. Hirata performed data analysis on the chimeric mice and cells. K. Ikeda, M. Ohta, T. Soga, and R. Taguchi performed data analysis on the result of MS spectrometry. A. Suzuki, K. Shimotohno, and M. Nishijima provided tools and expert information.

References

1. Wenk MR (2006) Lipidomics of host-pathogen interactions. FEBS Lett 580: 5541–5551.
2. Brown DA, Rose JK (1992) Sorting of GPI-anchored proteins to glycolipid-enriched membrane subdomains during transport to the apical cell surface. Cell 68: 533–544.
3. Simons K, Toomre D (2000) Lipid rafts and signal transduction. Nat Rev Mol Cell Biol 1: 31–39.
4. van der Meer-Janssen YP, van Galen J, Batenburg JJ, Helms JB (2010) Lipids in host-pathogen interactions: pathogens exploit the complexity of the host cell lipidome. Prog Lipid Res 49: 1–26.
5. Aizaki H, Lee KJ, Sung VM, Ishiko H, Lai MM (2004) Characterization of the hepatitis C virus RNA replication complex associated with lipid rafts. Virology 324: 450–461.
6. Shi ST, Lee KJ, Aizaki H, Hwang SB, Lai MM (2003) Hepatitis C virus RNA replication occurs on a detergent-resistant membrane that cofractionates with caveolin-2. J Virol 77: 4160–4168.
7. Sakamoto H, Okamoto K, Aoki M, Kato H, Katsume A, et al. (2005) Host sphingolipid biosynthesis as a target for hepatitis C virus therapy. Nat Chem Biol 1: 333–337.
8. Weng L, Hirata Y, Arai M, Kohara M, Wakita T, et al. (2010) Sphingomyelin activates hepatitis C virus RNA polymerase in a genotype-specific manner. J Virol 84: 11761–11770.
9. Umehara T, Sudoh M, Yasui F, Matsuda C, Hayashi Y, et al. (2006) Serine palmitoyltransferase inhibitor suppresses HCV replication in a mouse model. Biochem Biophys Res Commun 346: 67–73.
10. Kapadia SB, Chisari FV (2005) Hepatitis C virus RNA replication is regulated by host geranylgeranylation and fatty acids. Proc Natl Acad Sci U S A 102: 2561–2566.
11. Su AI, Pezacki JP, Wodicka L, Brideau AD, Supekova L, et al. (2002) Genomic analysis of the host response to hepatitis C virus infection. Proc Natl Acad Sci U S A 99: 15669–15674.
12. Takano T, Tsukiyama-Kohara K, Hayashi M, Hirata Y, Satoh M, et al. (2011) Augmentation of DHCR24 expression by hepatitis C virus infection facilitates viral replication in hepatocytes. J Hepatol 55: 512–521.
13. Tateno C, Yoshizane Y, Saito N, Kataoka M, Utoh R, et al. (2004) Near completely humanized liver in mice shows human-type metabolic responses to drugs. Am J Pathol 165: 901–912.
14. Mercer DF, Schiller DE, Elliott JF, Douglas DN, Hao C, et al. (2001) Hepatitis C virus replication in mice with chimeric human livers. Nat Med 7: 927–933.

15. Valsecchi M, Mauri L, Casellato R, Prioni S, Loberto N, et al. (2007) Ceramide and sphingomyelin species of fibroblasts and neurons in culture. J Lipid Res 48: 417–424.
16. Watanabe T, Sudoh M, Miyagishi M, Akashi H, Arai M, et al. (2006) Intracellular-diced dsRNA has enhanced efficacy for silencing HCV RNA and overcomes variation in the viral genotype. Gene Ther 13: 883–892.
17. Fujita T, Inoue K, Yamamoto S, Ikumoto T, Sasaki S, et al. (1994) Fungal metabolites. Part 11. A potent immunosuppressive activity found in Isaria sinclairii metabolite. J Antibiot (Tokyo) 47: 208–215.
18. Miyake Y, Kozutsumi Y, Nakamura S, Fujita T, Kawasaki T (1995) Serine palmitoyltransferase is the primary target of a sphingosine-like immunosuppressant, ISP-1/myriocin. Biochem Biophys Res Commun 211: 396–403.
19. Park TS, Panek RL, Mueller SB, Hanselman JC, Rosebury WS, et al. (2004) Inhibition of sphingomyelin synthesis reduces atherogenesis in apolipoprotein E-knockout mice. Circulation 110: 3465–3471.
20. Miyanari Y, Hijikata M, Yamaji M, Hosaka M, Takahashi H, et al. (2003) Hepatitis C virus non-structural proteins in the probable membranous compartment function in viral genome replication. J Biol Chem 278: 50301–50308.
21. Diamond DL, Jacobs JM, Paeper B, Proll SC, Gritsenko MA, et al. (2007) Proteomic profiling of human liver biopsies: hepatitis C virus-induced fibrosis and mitochondrial dysfunction. Hepatology 46: 649–657.
22. Tardif KD, Mori K, Siddiqui A (2002) Hepatitis C virus subgenomic replicons induce endoplasmic reticulum stress activating an intracellular signaling pathway. J Virol 76: 7453–7459.
23. Pettus BJ, Chalfant CE, Hannun YA (2002) Ceramide in apoptosis: an overview and current perspectives. Biochim Biophys Acta 1585: 114–125.
24. Tepper AD, Ruurs P, Wiedmer T, Sims PJ, Borst J, et al. (2000) Sphingomyelin hydrolysis to ceramide during the execution phase of apoptosis results from phospholipid scrambling and alters cell-surface morphology. J Cell Biol 150: 155–164.
25. Liu YY, Han TY, Giuliano AE, Hansen N, Cabot MC (2000) Uncoupling ceramide glycosylation by transfection of glucosylceramide synthase antisense reverses adriamycin resistance. J Biol Chem 275: 7138–7143.
26. Taguchi Y, Kondo T, Watanabe M, Miyaji M, Umehara H, et al. (2004) Interleukin-2-induced survival of natural killer (NK) cells involving phosphatidylinositol-3 kinase-dependent reduction of ceramide through acid sphingomyelinase, sphingomyelin synthase, and glucosylceramide synthase. Blood 104: 3285–3293.
27. Diamond DL, Syder AJ, Jacobs JM, Sorensen CM, Walters KA, et al. (2010) Temporal proteome and lipidome profiles reveal hepatitis C virus-associated reprogramming of hepatocellular metabolism and bioenergetics. PLoS Pathog 6: e1000719.
28. Huitema K, van den Dikkenberg J, Brouwers JF, Holthuis JC (2004) Identification of a family of animal sphingomyelin synthases. EMBO J 23: 33–44.
29. Merrill AH, Jr., Schmelz EM, Dillehay DL, Spiegel S, Shayman JA, et al. (1997) Sphingolipids–the enigmatic lipid class: biochemistry, physiology, and pathophysiology. Toxicol Appl Pharmacol 142: 208–225.
30. Huwiler A, Kolter T, Pfeilschifter J, Sandhoff K (2000) Physiology and pathophysiology of sphingolipid metabolism and signaling. Biochim Biophys Acta 1485: 63–99.
31. Hannun YA, Luberto C, Argraves KM (2001) Enzymes of sphingolipid metabolism: from modular to integrative signaling. Biochemistry 40: 4893–4903.
32. van Genderen IL, Brandimarti R, Torrisi MR, Campadelli G, van Meer G (1994) The phospholipid composition of extracellular herpes simplex virions differs from that of host cell nuclei. Virology 200: 831–836.
33. Brugger B, Glass B, Haberkant P, Leibrecht I, Wieland FT, et al. (2006) The HIV lipidome: a raft with an unusual composition. Proc Natl Acad Sci U S A 103: 2641–2646.
34. Aizaki H, Morikawa K, Fukasawa M, Hara H, Inoue Y, et al. (2008) Critical role of virion-associated cholesterol and sphingolipid in hepatitis C virus infection. J Virol 82: 5715–5724.
35. Syed GH, Amako Y, Siddiqui A (2010) Hepatitis C virus hijacks host lipid metabolism. Trends Endocrinol Metab 21: 33–40.
36. Berger KL, Cooper JD, Heaton NS, Yoon R, Oakland TE, et al. (2009) Roles for endocytic trafficking and phosphatidylinositol 4-kinase III alpha in hepatitis C virus replication. Proc Natl Acad Sci U S A 106: 7577–7582.
37. Borawski J, Troke P, Puyang X, Gibaja V, Zhao S, et al. (2009) Class III phosphatidylinositol 4-kinase alpha and beta are novel host factor regulators of hepatitis C virus replication. J Virol 83: 10058–10074.
38. Tai AW, Benita Y, Peng LF, Kim SS, Sakamoto N, et al. (2009) A functional genomic screen identifies cellular cofactors of hepatitis C virus replication. Cell Host Microbe 5: 298–307.
39. Vaillancourt FH, Pilote L, Cartier M, Lippens J, Liuzzi M, et al. (2009) Identification of a lipid kinase as a host factor involved in hepatitis C virus RNA replication. Virology 387: 5–10.
40. Amemiya F, Maekawa S, Itakura Y, Kanayama A, Matsui A, et al. (2008) Targeting lipid metabolism in the treatment of hepatitis C virus infection. J Infect Dis 197: 361–370.
41. Ishitsuka R, Sato SB, Kobayashi T (2005) Imaging lipid rafts. J Biochem 137: 249–254.
42. Ramstedt B, Slotte JP (2002) Membrane properties of sphingomyelins. FEBS Lett 531: 33–37.
43. He Q, Suzuki H, Sharma N, Sharma RP (2006) Ceramide synthase inhibition by fumonisin B1 treatment activates sphingolipid-metabolizing systems in mouse liver. Toxicol Sci 94: 388–397.
44. Bligh EG, Dyer WJ (1959) A rapid method of total lipid extraction and purification. Can J Biochem Physiol 37: 911–917.
45. Inoue K, Umehara T, Ruegg UT, Yasui F, Watanabe T, et al. (2007) Evaluation of a cyclophilin inhibitor in hepatitis C virus-infected chimeric mice in vivo. Hepatology 45: 921–928.
46. Kashiwakuma T, Hasegawa A, Kajita T, Takata A, Mori H, et al. (1996) Detection of hepatitis C virus specific core protein in serum of patients by a sensitive fluorescence enzyme immunoassay (FEIA). J Immunol Methods 190: 79–89.
47. Ikeda K, Shimizu T, Taguchi R (2008) Targeted analysis of ganglioside and sulfatide molecular species by LC/ESI-MS/MS with theoretically expanded multiple reaction monitoring. J Lipid Res 49: 2678–2689.
48. Taguchi R, Nishijima M, Shimizu T (2007) Basic analytical systems for lipidomics by mass spectrometry in Japan. Methods Enzymol 432: 185–211.
49. Ikeda K, Oike Y, Shimizu T, Taguchi R (2009) Global analysis of triacylglycerols including oxidized molecular species by reverse-phase high resolution LC/ESI-QTOF MS/MS. J Chromatogr B Analyt Technol Biomed Life Sci 877: 2639–2647.
50. Ikeda K, Mutoh M, Teraoka N, Nakanishi H, Wakabayashi K, et al. (2011) Increase of oxidant-related triglycerides and phosphatidylcholines in serum and small intestinal mucosa during development of intestinal polyp formation in Min mice. Cancer Sci 102: 79–87.

Biochemical and Biophysical Research Communications 428 (2012) 494–499

Contents lists available at SciVerse ScienceDirect

Biochemical and Biophysical Research Communications

journal homepage: www.elsevier.com/locate/ybbrc

Impairment of interferon regulatory factor-3 activation by hepatitis C virus core protein basic amino acid region 1

Kazuaki Inoue [a,b], Kyoko Tsukiyama-Kohara [a,c,d], Chiho Matsuda [a], Mitsutoshi Yoneyama [e], Takashi Fujita [f], Shusuke Kuge [g], Makoto Yoshiba [b], Michinori Kohara [a,*]

[a] Department of Microbiology and Cell Biology, The Tokyo Metropolitan Institute of Medical Science, 2-1-6 Kamikitazawa, Setagaya-ku, Tokyo 156-0057, Japan
[b] Division of Gastroenterology, Showa University Fujigaoka Hospital, 1-30 Aoba-ku, Fujigaoka, Yokohama 227-8501, Japan
[c] Department of Experimental Phylaxiology, Faculty of Life Sciences, Kumamoto University, 1-1-1 Honjo, Kumamoto City, Kumamoto 860-8556, Japan
[d] Joint Faculty of Veterinary Medicine, Kagoshima University, 1-21-24 Korimoto, Kagoshima City, Kagoshima 890-0065, Japan
[e] Medical Microbiology Research Center, Chiba University, 1-8-1 Inohana Chuo-Ku, Chiba-City, Chiba 260-8673, Japan
[f] Laboratory of Molecular Genetics, Institute for Virus Research, Kyoto University, Kyoto 606-8507, Japan
[g] Laboratory of Microbiology, Tohoku Pharmaceutical University, Komatsushima, Aoba-ku, Sendai 981-8558, Japan

ARTICLE INFO

Article history:
Received 17 October 2012
Available online 30 October 2012

Keywords:
Hepatitis C virus
IRF-3
Core protein
Type I interferon signaling
Basic amino acid region 1
Interferon beta

ABSTRACT

Interferon regulatory factor-3 (IRF-3), a key transcriptional factor in the type I interferon system, is frequently impaired by hepatitis C virus (HCV), in order to establish persistent infection. However, the exact mechanism by which the virus establishes persistent infection has not been fully understood yet. The present study aimed to investigate the effects of various HCV proteins on IRF-3 activation, and elucidate the underlying mechanisms. To achieve this, full-length HCV and HCV subgenomic constructs corresponding to structural and each of the nonstructural proteins were transiently transfected into HepG2 cells. IFN-β induction, plaque formation, and IRF-3 dimerization were elicited by Newcastle disease virus (NDV) infection. The expressions of IRF-3 homodimer and its monomer, Ser386-phosphorylated IRF-3, and HCV core protein were detected by immunofluorescence and western blotting. IFN-β mRNA expression was quantified by real-time PCR (RT-PCR), and IRF-3 activity was measured by the levels of IRF-3 dimerization and phosphorylation, induced by NDV infection or polyriboinosinic:polyribocytidylic acid [poly(I:C)]. Switching of the expression of the complete HCV genome as well as the core proteins, E1, E2, and NS2, suppressed IFN-β mRNA levels and IRF-3 dimerization, induced by NDV infection. Our study revealed a crucial region of the HCV core protein, basic amino acid region 1 (BR1), to inhibit IRF-3 dimerization as well as its phosphorylation induced by NDV infection and poly (I:C), thus interfering with IRF-3 activation. Therefore, our study suggests that rescue of the IRF-3 pathway impairment may be an effective treatment for HCV infection.

1. Introduction

Hepatitis C virus (HCV), a flavivirus comprising a positive-sense, single-stranded RNA (ssRNA) of approximately 9.6 kb [1], causes persistent disease in infected individuals, possibly leading to chronic liver injury [2]. Despite the approximately 170 million individuals worldwide suffering from HCV infection that ranges from chronic hepatitis to hepatocellular carcinoma (HCC) [3,4], the exact mechanism by which the virus establishes persistent infection is not fully resolved.

The innate immune system is activated immediately upon infection as the first line of host defense against invading pathogens, with type I interferon (IFN) signaling being the crucial step in the antiviral response [5]. The IFN system is, therefore, a prime target of HCV and other viruses in order to establish persistent infections [6], wherein the disruption of the type I IFN-activation pathway forms the most efficient strategy for HCV. Studies on HCV IFN-interference mechanisms have revealed that the HCV proteins NS5A and E2 selectively inhibit the double-stranded RNA-activated protein kinase (PKR) [7,8], an IFN-inducible antiviral molecule that controls transcription and translation [6]. IFN-β, a crucial molecule in type I IFN signaling, is regulated by several cellular factors associated with the activation of interferon regulatory factor-3 (IRF-3), leading to its rapid induction following viral infection [9,10]. However, IFN-β induction is impaired in HCV-infected cells, thus resulting in the disruption of IFN downstream signaling cascade [11].

IRF-3, a key constitutively expressed transcriptional factor localized in the cytoplasm in its inactive form [9], is activated upon

* Corresponding author. Fax: +81 3 5316 3137.
E-mail address: kohara-mc@igakuken.or.jp (M. Kohara).

0006-291X/$ - see front matter © 2012 Elsevier Inc. All rights reserved.
http://dx.doi.org/10.1016/j.bbrc.2012.10.079

phosphorylation, whereby it translocates to the nucleus to act as a transcriptional factor for positive regulatory domain (PRD) I of the IFN-β promoter. IRF-3 activation also induces phosphorylation of Ser385 and Ser386 or the serine/threonine (Ser/Thr) cluster between amino acids (aa) 396 and 405 (located at the C-terminus of IRF-3), a step that is essential for dimerization and nuclear translocation.

A previous study by Foy et al. showed that the NS3/4A serine protease derived from a subgenomic replicon participates in the suppression of the cellular pathway that activates IRF-3 [12]. The NS3/4A protein of HCV disrupts signaling of the double-stranded RNA (dsRNA) receptors, retinoic acid-inducible gene-I (RIG-I), and Toll-like receptor 3 (TLR3) by inducing proteolysis of interferon promoter stimulator-1 (IPS-1) [13–15] and Toll/interleukin-1 receptor (TIR) domain-containing adaptor protein inducing IFN-β (TRIF) [16], as well as by suppressing the downstream activation of IFN-β [13].

In view of the above observations and the emerging data on the role of HCV in regulating the IRF-3 pathway by additional mechanisms, we aimed to investigate the effects of various HCV proteins on IRF-3 activation, and further elucidate the underlying novel mechanisms.

2. Material and methods

2.1. Transient expression of the HCV core proteins E1, E2, and NS3-4A

HepG2 cells were transfected to express E1, E2, or NS3-4A HCV core protein under the control of EF promoter (Invitrogen). The HCV core expression vectors were derived from HCR6 (genotype 1b), HCR24-12K (genotype 2a), or HCR24-12Q (genotype 2a). The E1, E2, and NS3 clones derived from HCR6 contained either the full-length cDNAs encoding the core protein or 1 of the 3 different deletions (deletion mutants), each of which lacked 1 of the 3 basic amino acid regions (BR), BR1 deletion (aa 4–14), BR2 deletion (aa 37–44), and BR3 deletion (aa 57–72) [17]. HepG2 cells were transfected with 4 μg of the core cDNA (amino acids 1–191), E1 (amino

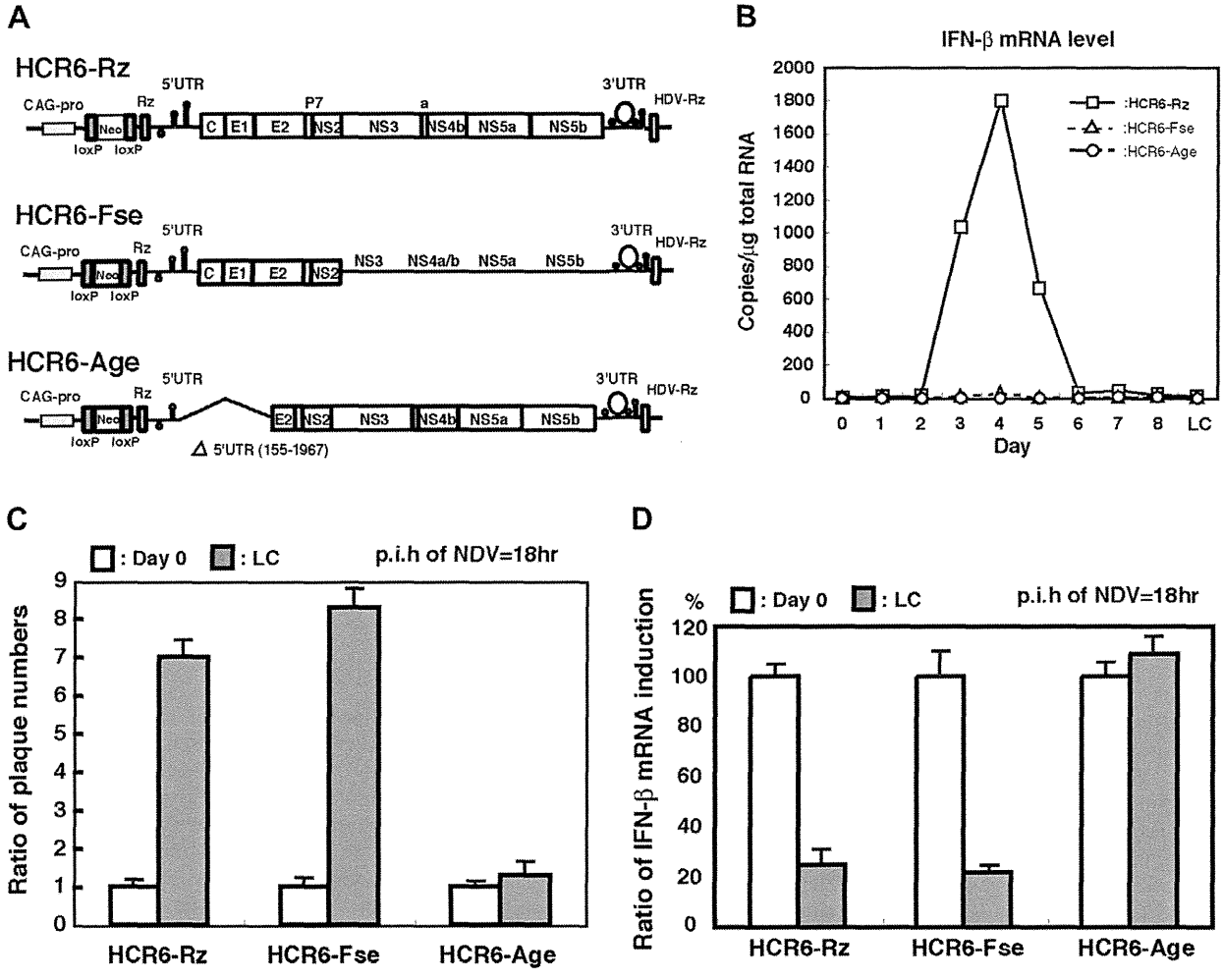

Fig. 1. (A) Structures of the conditional expression vectors for HCV RNAs and proteins. The cDNA clones that displayed highest level of homology to the consensus sequences among the 3 clones were used to construct *HCR6-Rz* (nt 1–9611). *HCR6-Fse* clone harbored a termination codon introduced at nucleotide 3606 and truncated *HCR6-Age* clone lacked nucleotides 155–1967. They were flanked with ribozyme (Rz) and hepatitis D virus ribozyme (HDV-Rz) sequences under the control of the CAG promoter in the Cre/*loxP* switching expression cassette, which consisted of the neomycin resistance gene, as a stuffer region flanked by the *loxP* sequence. (B) IFN-β mRNA levels in the cell lines *HCR6-Rz*, *HCR6-Fse*, and *HCR6-Age* before and after the expression of the HCV protein. The results are expressed as copy numbers per microgram of total RNA, as quantified by RT-PCR. (C) Efficiency of NDV plaque formation. Plaque assays were performed on Vero cells for NDV infectivity in *HCR6-Rz*, *HCR6-Fse*, or *HCR6-Age* before and after the expression of the HCV protein. The plaque numbers were counted 3 days after NDV inoculation. The ratio indicates the plaque numbers after the expression of the HCV genome divided by the plaque numbers before the expression of the HCV genome. (D) Suppression of IFN-β mRNA induction by HCV expression, 18 days after NDV inoculation. Day 0, before the expression of the HCV genome; Day 48, after the expression of the HCV genome. The results are expressed relative to the levels on Day 0 (100%) in each of the 3 HCV-expressing systems. p.i.h., post-inoculation hour.

acids 192–383), E2 (amino acids 384–809), NS3-4A (amino acids 1027–1711), or the core regions lacking the BR, in 35-mm dishes, by using Lipofectamine 2000 (Invitrogen) at 37 °C for 6 h. The medium was subsequently replaced with normal culture medium, and the cells were harvested after 48 h.

2.2. Newcastle disease virus (NDV) infection and addition of polyriboinosinic:polyribocytidylic acid [poly(I:C)]

NDV (Miyadera strain) was propagated from swabs by using the embryonated egg culture method, as described in the Supplementary methods.

Poly(I:C) (20 μg/well; GE Healthcare) was added to HepG2 cells in 35-mm dishes, 48 h after transfection with the core expression vector derived from HCR6 (genotype 1b).

2.3. Native PAGE of IRF-3 and phosphorylated IRF-3

Cells were lysed in 30 μL of lysis buffer (50 mM Tris–HCl [pH 8.0], 1% NP-40, 150 mM NaCl, 100 μg/mL leupeptin, 1 mM PMSF, 5 mM Na_3VO_4), mixed vigorously, and centrifuged at 15,000 rpm for 10 min; the supernatant was isolated. Total protein samples (10 μg) were electrophoresed on a 7.5% native PAGE gel (Bio-Rad Laboratories) and transferred onto a PVDF membrane. IRF-3 homodimer and its monomer and Ser386-phosphorylated IRF-3 were detected by western blotting using polyclonal rabbit antibodies, anti-human IRF-3 (1:1000) [18] and, anti-human Ser386-phosphorylated IRF-3 (1:10,000), respectively. Detection was achieved by enhanced chemiluminescence (ECL; Amersham, UK) according to the manufacturer's instructions. The rabbit anti-human IRF-3 and anti-human Ser386-phosphorylated IRF-3 antibodies were described previously [19].

2.4. Quantification of IFN-β gene expression

IFN-β mRNA expression was quantified by using real-time PCR (RT-PCR) as described previously [20] and Supplementary methods using the following primers and probes: sense (5′-CCATCTATGA GATGCTCCAGAA-3′), antisense (5′-TTTTCTTCCAGGACTGTCTTCA-GA-3′) and probe (5′-AGCACTGGCTGGAATGAGACTATTGTTG-3′).

3. Results

3.1. Induction of IFN and IRF-3 by HCV-Rz

To evaluate the effect of HCV gene persistent expression, cell lines expressing the HCV genomes in a Cre/*lox*P expression system [20] were established by transfecting the full-genome HCV (*HCR6-Rz*); core, E1, E2, and NS2 (*HCR6-Fse*); and E2~NS5b (*HCR6-Age*) (Fig. 1A) clones into HepG2 cells. Of the 3 HCV expression systems, only *HCR6-Rz* transiently induced endogenous IFN-β expression (Fig. 1B). No endogenous IFN-β was detected by RT-PCR on Day 0 or Day 48 (long culture; LC) [21] in any of the 3 systems (Fig. 1B).

3.2. Effect of HCV expression on NDV infection and IFN-β induction

Further, we examined whether the persistent expression of HCV genome influenced the plaque formation activity of NDV in *HCR6-Rz*-, *HCR6-Fse*-, and *HCR6-Age*-expressing cell lines. Prior to the expression of HCV proteins, the plaque numbers were similar across all the cell lines (Fig. 1C). Expression of HCV proteins for more than 48 days [21] increased plaque numbers in the *HCR6-Rz*- and *HCR6-Fse*-expressing cells from 7- to 8-fold (Fig. 1C); however, plaque numbers in the *HCR6-Age*-expressing cells remained constant. These findings thus indicate that HCV structural proteins interfered with the induction of IFN-β mRNA, after NDV infection (18 h post-infection). Therefore, we measured IFN-β mRNA levels in the 3 cell lines, *HCR6-Rz*, *HCR6-Fse*, and *HCR6-Age*, by RT-PCR before (Day 0) and after (Day 48) inoculation with NDV (Fig. 1D). The mRNA expression of IFN-β was not observed prior to NDV infection in any of the 3 cell lines (Day 0). Notably, after 18 h of NDV inoculation and prior to the expression of various HCV proteins (Day 0), the levels of IFN-β mRNA transcription were similar among *HCR6-Rz*-, *HCR6-Fse*-, and *HCR6-Age*-expressing cell lines (Fig. 1D). Following HCV protein expression, the induced IFN-β mRNA expression was reduced to 20% in both *HCR6-Rz*- and *HCR6-Fse*-expressing cell lines. However, IFN-β mRNA expression remained constant in the *HCR6-Age*-expressing cell line.

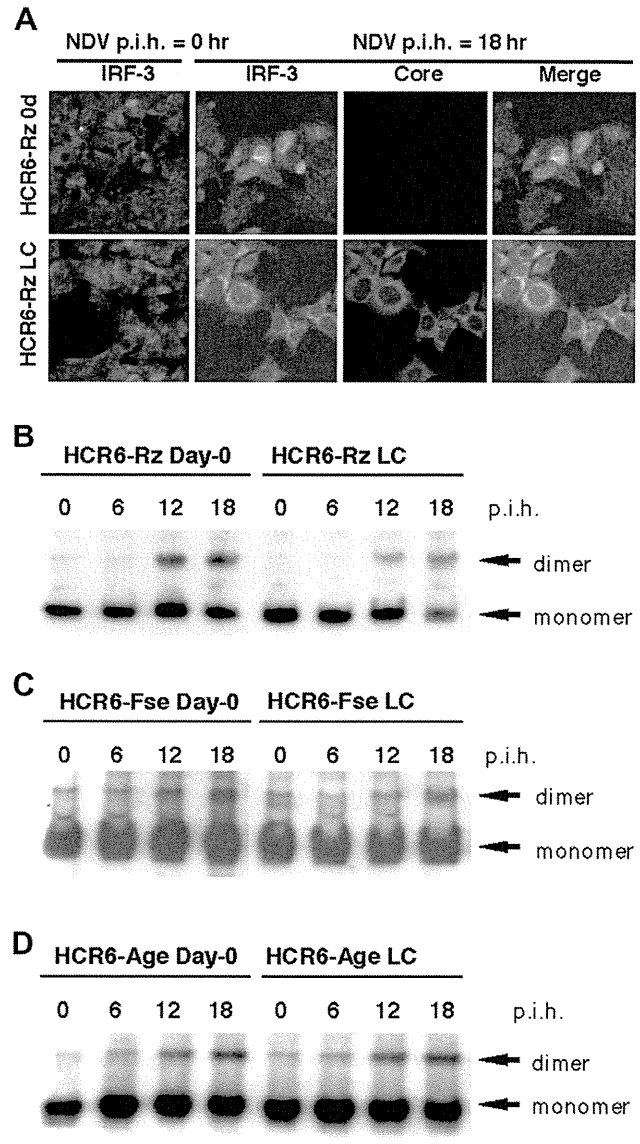

Fig. 2. (A) HCV inhibition of IRF-3 nuclear translocation. IRF-3 is a constitutively expressed transcriptional factor that localizes in the cytoplasm in a diffuse manner, when inactive. After NDV inoculation and prior to the expression of the HCV genome, IRF-3 translocated to the nucleus but was retained at a perinuclear site in the *HCR6-Rz*-expressing cells (Day 48). IRF-3 colocalized with the HCV core protein. (B–D) Suppression of IRF-3 dimerization by HCV expression. The dimeric and monomeric forms of IRF-3 were detected by western blotting on native PAGE gels. The influence of (B) *HCR6-Rz* expression, (C) *HCR6-Fse* expression, and (D) *HCR6-Age* expression on IRF-3 dimerization is shown. NDV was used to induce IRF-3 dimerization.

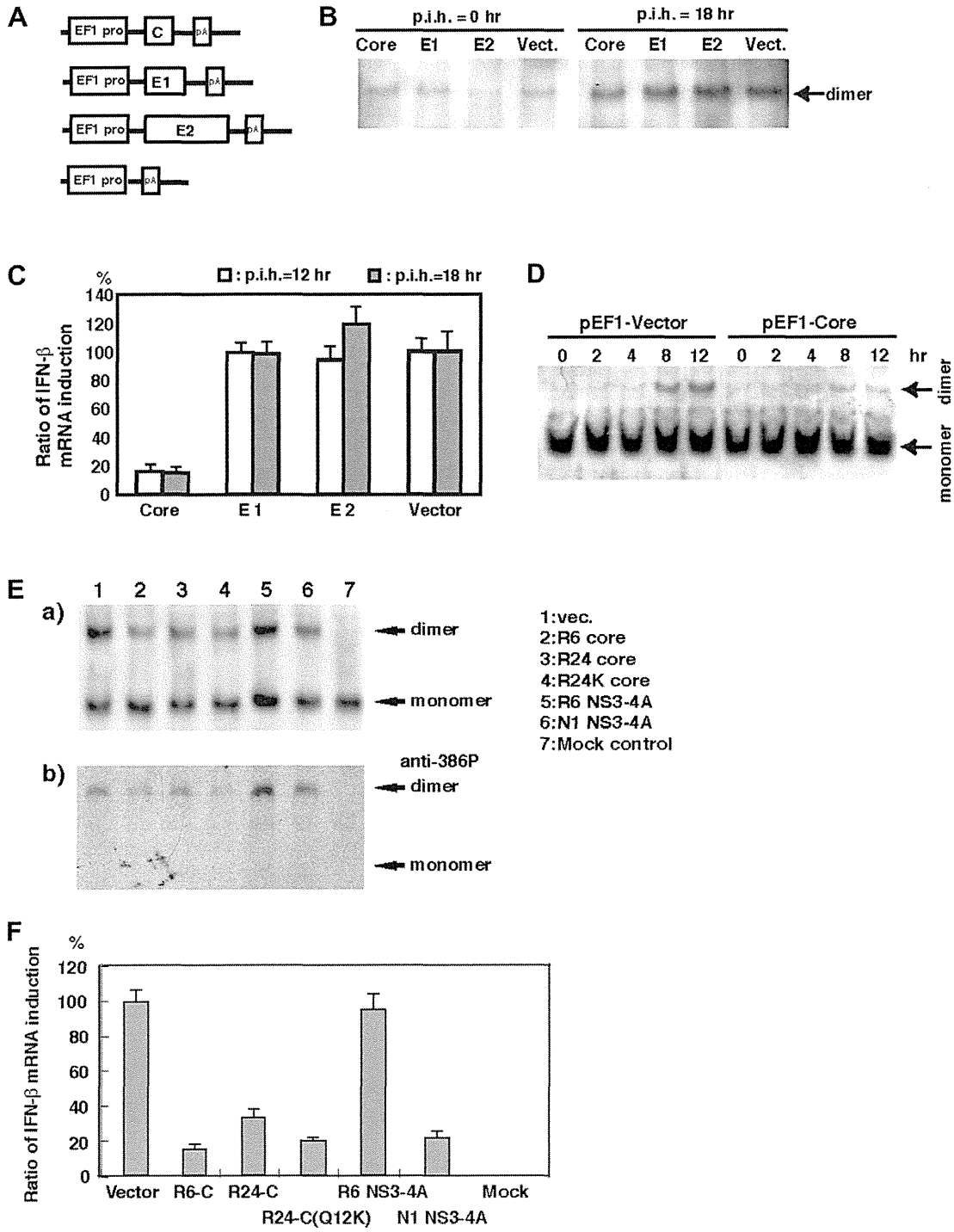

Fig. 3. (A) Structures of the HCR6 core, E1, and E2 expression vectors encoding the HCV core (aa 1–191), E1 (amino acids 192–383), and E2 (amino acids 384–809) proteins, respectively, under the control of the EF1 promoter. (B) Left panel, IRF-3 dimerization induced by NDV before transfection with the expression vectors; right panel, IRF-3 dimerization induced by NDV after transfection with the expression vectors. (C) IFN-β mRNA induction levels at 12 and 18 h after NDV inoculation into HepG2 cells transfected with the vector alone, core, E1, or E2 proteins. The results are expressed relative to the induction levels of IFN-β in HepG2 cells transfected with the vector alone (100%), for post-inoculation, each time. (D) IRF-3 dimerization on administration of 10 mg/mL poly(I:C) before the expression (Day 0), and at 2, 4, 8, and 12 h after the expression of the HCV core (pEF-Core) or vector plasmid DNA. (E) Effects of the expression of vector (lane 1), R6 core (lane 2), R24 core (lane 3), R24 core (Q12K) (lane 4), R6-NS3-4A (lane 5), N1-NS3-4A (lane 6), and mock control (lane 7) on IRF-3 dimerization (upper column a) and phosphorylation of serine residue at amino acid 386 in IRF-3 (lower column b), after infection with NDV for 18 h. F. Effects of the expressions of R6-C, R24-C, R24-C(Q12K), and R6-NS3 on IFN-β induction, 18 h after NDV inoculation. The IFN-β mRNA levels were assayed by RT-PCR. The results are expressed relative to the induction levels of IFN-β in HepG2 cells transfected with the vector alone (100%).

3.3. Effect of HCV on IRF-3 localization, nuclear translocation, and dimerization by NDV

The effect of HCV expression on cellular localization of IRF-3 was analyzed in *HCR6-Rz*-expressing cells infected with NDV before (Day 0) and after LC (Fig. 2A). Prior to NDV infection, IRF-3 was detected in the cytoplasm by immunofluorescence. Notably, after 18 h of NDV inoculation and prior to *HCR6-Rz* protein expression, when IFN-β induction and IRF-3 dimerization were maximal, a substantial amount of IRF-3 translocated to the nucleus.

However, this nuclear translocation was suppressed in the presence of HCV proteins (Fig. 2A) and resulted in the co-localization of the HCV core protein with IRF-3 at perinuclear sites (Fig. 2A, superimposed image of IRF-3 and core protein immunostaining).

To elucidate the mechanism underlying the suppression of IFN-β mRNA in *HCR6-Rz*- and *HCR6-Fse*-expressing cells, we examined the effect of HCV expression on IRF-3 dimerization after NDV infection (Fig. 2B). Interestingly, the levels of IRF-3 dimerization peaked at 12–18 h after NDV infection in the 3 cell lines lacking HCV expression (Day 0; Fig. 2). However, in the *HCR6-Rz*- and *HCR6-Fse*-expressing cell lines, IRF-3 dimerization was found to be significantly reduced, (Fig. 2B and C) when compared to that in the *HCR6-Age*-expressing cells (Fig. 2D).

3.4. Identification of the HCV genome region responsible for the inhibition of IRF-3 dimerization and IFN-β induction

To identify the HCV genome region responsible for suppression of IRF-3 dimerization, HepG2 cells were transfected to express the HCV core regions derived from HCR6, E1, or E2 (genotype 1b; Fig. 3A). Protein expression was confirmed by western blotting (data not shown). The HCV core protein suppressed IRF-3 dimerization, but E1 and E2 expressions had no effect on the dimerization (Fig. 3B). Expression of E1, E2, or the vector alone did not alter the levels of IFN-β mRNA induced by NDV infection in HepG2 cells (Fig. 3C), but significantly reduced IFN-β mRNA levels at both 12 and 18 h after infection (Fig. 3C).

3.5. Effect of HCV core protein expression on IRF-3 dimerization through TLR3

Among the synthetic dsRNAs, poly(I:C) is a potent inducer of IFN-β through TLR3. Accordingly, HepG2 cells transfected with poly(I:C) and the vector control (pEF1-vector) showed IRF-3 dimerization (Fig. 3D). In contrast, IRF-3 dimerization was suppressed in HepG2 cells expressing the HCV core protein albeit the induction of IFN-β mRNA following poly(I:C) expression (data not shown).

3.6. Effect of the HCV core protein NS3 and core proteins derived from genotype 2a on IRF-3 dimerization, compared to proteins derived from genotype 1b

Further, we investigated whether the HCV core protein NS3 and core proteins derived from other genotypes exerted the same effects on IRF-3 after 18 h of NDV infection. The core proteins derived from genotypes 1b (R6) and 2a (R24-12Q and R24-12K) suppressed IRF-3 dimerization in cells infected with NDV (Fig. 3E(a)). In contrast, IRF-3 dimerization remained unaltered in the presence of R6 clone NS3 protein, but was suppressed by the N clone NS3 protein. Thus, NS3-4A protein of R6 clone suppressed IRF-3 dimerization to a relatively lesser extent compared to that of the N1 strain. Similar results were obtained for the phosphorylation at Ser386 in IRF-3 (Fig. 3E(b)). The IFN-β mRNA transcription was quantified in HepG2 cells by RT-PCR after transfection with these expression vectors (Fig. 3F).

3.7. Identification of the HCV core region responsible for suppressing IRF-3 dimerization

We sought to identify the region of the HCV core protein responsible for suppressing IRF-3 dimerization. Expression vectors encoding the entire HCV core or the core region lacking 1 of the 3 basic amino acid regions (BR) that influenced nuclear translocation [17] were transfected into HepG2 cells, and the effects on IRF-3 dimerization were examined (Fig. 4A). Protein

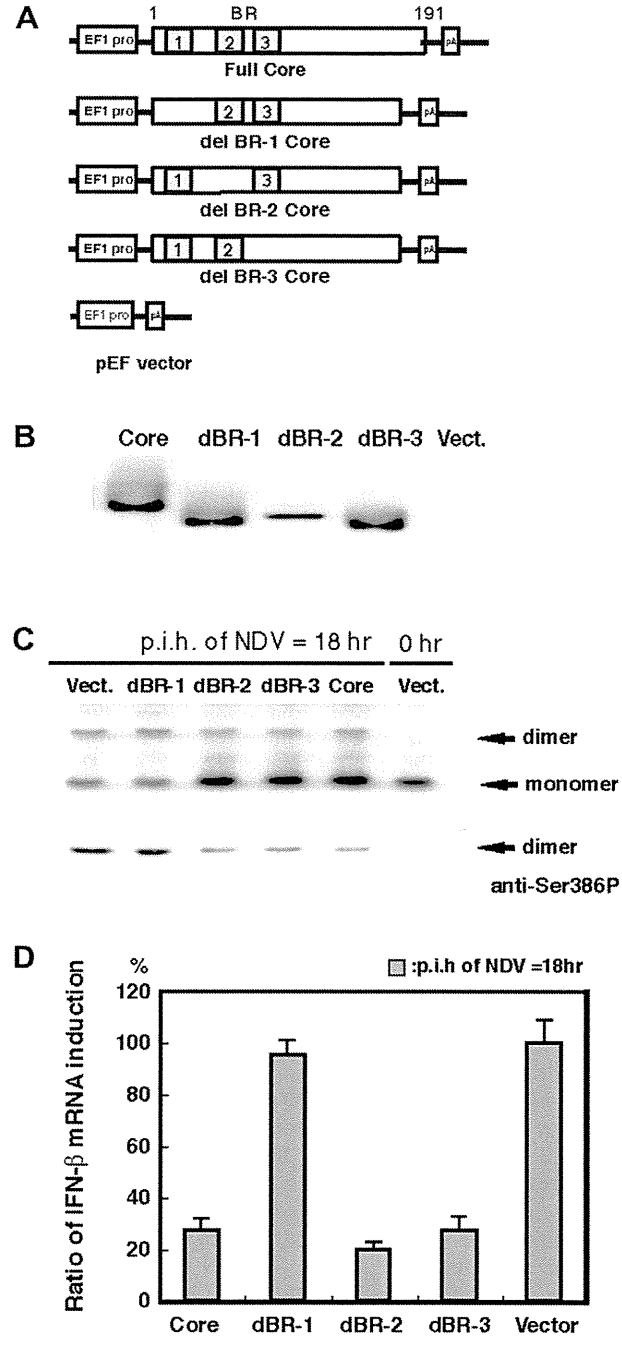

Fig. 4. (A) Structures of the HCR6 core, E1, and E2 expression vectors carrying the complete core, BR1 deletion (aa 4–14), BR2 deletion (aa 37–44), and BR3 deletion (aa 57–72). (B) Western blotting to confirmed the expression of the mutated core proteins. (C) Effects of the expression of various mutated core proteins on IRF-3 dimerization and IRF-3 phosphorylation at Ser386, 18 h after NDV inoculation. (D) Effects of the expression of each type of core protein region on IFN-β mRNA synthesis, 18 h after NDV inoculation. The results are expressed relative to the induction levels of IFN-β in HepG2 cells transfected with the vector alone (100%). IFN-β mRNA levels were assayed by RT-PCR.

expression of the core and the deletion mutants (BR1, BR2, and BR3) was confirmed by western blotting (Fig. 4B). IRF-3 dimerization, phosphorylation at Ser386 of IRF-3, and induction of IFN-β mRNA were suppressed in HepG2 cells expressing the entire core, a deletion of BR2, or a deletion of BR3 (Fig. 4C), but not in cells expressing the BR1-deleted HCV core regions (Fig. 4C and D).

4. Discussion

The present study indicates that the HCV core protein inhibits IRF-3 dimerization, IRF-3 phosphorylation at Ser386, and IFN-β induction. In addition, our study showed that the effect of the core protein derived from genotype 1b was similar to that of the core protein derived from genotype 2a, indicating that the inhibitory effect of the core protein might be effective in several genotypes of HCV. These findings are corroborated by a previous study by Foy et al. [12] who showed that HCV NS3/4 disrupts virus-associated-kinase-mediated IRF-3 activation, which further results in the suppression of IRF-3 phosphorylation, nuclear translocation, and IRF-3-dependent ISRE/PRDI activation. These findings indicate that attenuation of the IFN system was achieved through NS3/4A proteins via the interference of IRF-3 activation, thus strengthening our results, which show the potential of HCV core protein to interfere with IRF-3 activation in promoting persistent infection.

Furthermore, the present study showed that the N-terminal region of the core protein and BR-1 domain in particular are responsible for inactivating IRF-3. The N-terminal region (amino acids 1–59) of the HCV core protein has been identified as the binding region for a DEAD box protein (DDX3) [22]. Human DDX3, a putative RNA helicase, is a member of the highly conserved DEAD box subclass that includes the expression of murine PL10, *Xenopus* An3, and yeast Ded 1 proteins. Recently, expression of DDX3 was found to enhance IFN-β promoter induction by TBK1/IKKε, whereas silencing of DDX3 inhibited IFN-β promoter and virus- or dsRNA-induced IRF-3 activation [23]. It was shown that Vaccinia virus K7 protein also binds to DDX3 and inhibits pattern recognition receptor-induced IFN-β induction by preventing TBK1/IKKε-mediated IFN-β induction via impaired TBK1/IKKε-induced activation of IRF-3 [23]. A previous study by Oshiumi et al. showed that DDX3 C-terminal region (amino acids 622–662) directly binds to the IFN-beta promoter stimulator-1 (IPS-1) CARD-like domain [24] as well as the N-terminal HCV core protein [36]. The present study demonstrated that the expression of the core protein decreased the levels of DDX3 expression (data not shown). This is in agreement with the result of a previous study, which showed that DDX3 is downregulated in HCV-associated hepatocellular carcinoma (HCC) and silencing of DDX3 accelerates cell growth [25]. Collectively, these findings suggest that DDX3 may be the target of the core protein for inhibiting IRF-3 activation.

In conclusion, our study revealed a crucial region of the HCV core protein, basic amino acid region 1, to interfere with IRF-3 activation and thereby inhibit the IFN signaling cascades. Therefore, the inhibitory effects that result in the IRF-3 pathway impairment could be rescued by deleting the basic region 1 of core protein, thus suggesting that it might be an effective treatment for HCV infection. Future studies involving DDX3 modification by the HCV core protein may be interesting to explore the cell growth-dysregulation mechanisms.

Acknowledgments

This study was supported in part by a grant from the Ministry of Education, Culture, Sports, Science and Technology of Japan; a grant from the Ministry of Health, Labour and Welfare of Japan; and the Program for Promotion of Fundamental Studies in Health Sciences of the National Institute of Biomedical Innovation of Japan; and the Cooperative Research Project on Clinical and Epidemiological Studies of Emerging and Re-emerging Infectious Diseases.

Appendix A. Supplementary data

Supplementary data associated with this article can be found, in the online version, at http://dx.doi.org/10.1016/j.bbrc.2012.10.079.

References

[1] N. Kato, M. Hijikata, Y. Ootsuyama, et al., Molecular cloning of the human hepatitis C virus genome from Japanese patients with non-A, non-B hepatitis, Proc. Natl. Acad. Sci. USA 87 (1990) 9524–9528.
[2] L.B. Seeff, F.B. Hollinger, H.J. Alter, et al., Long-term mortality and morbidity of transfusion-associated non-A, non-B, and type C hepatitis: a National Heart, Lung, and Blood Institute collaborative study, Hepatology 33 (2001) 455–463.
[3] H.B. El-Serag, Hepatocellular carcinoma and hepatitis C in the United States, Hepatology 36 (2002) S74–S83.
[4] D. Thomas, The hepatitis C viruses, in: C. Hagedorn, C. Rice (Eds.), Hepatitis C Epidemiology, Springer-Verlag, Berlin, 1999, pp. 25–42.
[5] G.R. Foster, Interferons in host defense, Semin. Liver Dis. 17 (1997) 287–295.
[6] R. Kaufman, Translation control of genome expression, in: N Sonenberg, J Hershey, M Matthews (Eds.), The double strand RNA-activated protein kinase PKR, Cold Spring Harbor, New York, 2000, pp. 503–527.
[7] M.J. Gale Jr., M.J. Korth, N.M. Tang, et al., Evidence that hepatitis C virus resistance to interferon is mediated through repression of the PKR protein kinase by the nonstructural 5A protein, Virology 230 (1997) 217–227.
[8] D.R. Taylor, S.T. Shi, P.R. Romano, et al., Inhibition of the interferon-inducible protein kinase PKR by HCV E2 protein, Science 285 (1999) 107–110.
[9] M. Yoneyama, W. Suhara, Y. Fukuhara, et al., Direct triggering of the type I interferon system by virus infection: activation of a transcription factor complex containing IRF-3 and CBP/p300, Embo. J. 17 (1998) 1087–1095.
[10] J. Hiscott, Triggering the innate antiviral response through IRF-3 activation, J. Biol. Chem. 282 (2007) 15325–15329.
[11] E.F. Meurs, A. Breiman, The interferon inducing pathways and the hepatitis C virus, World J. Gastroenterol. 13 (2007) 2446–2454.
[12] E. Foy, K. Li, C. Wang, et al., Regulation of interferon regulatory factor-3 by the hepatitis C virus serine protease, Science 300 (2003) 1145–1148.
[13] E. Meylan, J. Curran, K. Hofmann, et al., Cardif is an adaptor protein in the RIG-I antiviral pathway and is targeted by hepatitis C virus, Nature 437 (2005) 1167–1172.
[14] X.D. Li, L. Sun, R.B. Seth, et al., Hepatitis C virus protease NS3/4A cleaves mitochondrial antiviral signaling protein off the mitochondria to evade innate immunity, Proc. Natl. Acad. Sci. USA 102 (2005) 17717–17722.
[15] R. Lin, J. Lacoste, P. Nakhaei, et al., Dissociation of a MAVS/IPS-1/VISA/Cardif-IKKepsilon molecular complex from the mitochondrial outer membrane by hepatitis C virus NS3-4A proteolytic cleavage, J. Virol. 80 (2006) 6072–6083.
[16] K. Li, E. Foy, J.C. Ferreon, et al., Immune evasion by hepatitis C virus NS3/4A protease-mediated cleavage of the Toll-like receptor 3 adaptor protein TRIF, Proc. Natl. Acad. Sci. USA 102 (2005) 2992–2997.
[17] R. Suzuki, Y. Matsuura, T. Suzuki, et al., Nuclear localization of the truncated hepatitis C virus core protein with its hydrophobic C terminus deleted, J. Gen. Virol. 76 (Pt 1) (1995) 53–61.
[18] W. Suhara, M. Yoneyama, I. Kitabayashi, et al., Direct involvement of CREB-binding protein/p300 in sequence-specific DNA binding of virus-activated interferon regulatory factor-3 holocomplex, J. Biol. Chem. 277 (2002) 22304–22313.
[19] M. Mori, M. Yoneyama, T. Ito, et al., Identification of Ser-386 of interferon regulatory factor 3 as critical target for inducible phosphorylation that determines activation, J. Biol. Chem. 279 (2004) 9698–9702.
[20] K. Tsukiyama-Kohara, S. Tone, I. Maruyama, et al., Activation of the CKI-CDK-Rb-E2F pathway in full genome hepatitis C virus-expressing cells, J. Biol. Chem. 279 (2004) 14531–14541.
[21] T. Nishimura, M. Kohara, K. Izumi, et al., Hepatitis C virus impairs p53 via persistent overexpression of 3beta-hydroxysterol Delta24-reductase, J. Biol. Chem. 284 (2009) 36442–36452.
[22] A.M. Owsianka, A.H. Patel, Hepatitis C virus core protein interacts with a human DEAD box protein DDX3, Virology 257 (1999) 330–340.
[23] M. Schroder, M. Baran, A.G. Bowie, Viral targeting of DEAD box protein 3 reveals its role in TBK1/IKKepsilon-mediated IRF activation, EMBO J. 27 (2008) 2147–2157.
[24] H. Oshiumi, K. Sakai, M. Matsumoto, T. Seya, DEAD/H BOX 3 (DDX3) helicase binds the RIG-I adaptor IPS-1 to up-regulate IFN-beta-inducing potential, Eur. J. Immunol. 40 (4) (2010) 940–948.
[25] P.C. Chang, C.W. Chi, G.Y. Chau, et al., DDX3, a DEAD box RNA helicase, is deregulated in hepatitis virus-associated hepatocellular carcinoma and is involved in cell growth control, Oncogene 25 (2006) 1991–2003.

PLOS ONE

Immunization with a Recombinant Vaccinia Virus That Encodes Nonstructural Proteins of the Hepatitis C Virus Suppresses Viral Protein Levels in Mouse Liver

Satoshi Sekiguchi[1], Kiminori Kimura[2], Tomoko Chiyo[1], Takahiro Ohtsuki[1], Yoshimi Tobita[1], Yuko Tokunaga[1], Fumihiko Yasui[1], Kyoko Tsukiyama-Kohara[3], Takaji Wakita[4], Toshiyuki Tanaka[5], Masayuki Miyasaka[6], Kyosuke Mizuno[7], Yukiko Hayashi[8], Tsunekazu Hishima[8], Kouji Matsushima[9], Michinori Kohara[1]*

1 Department of Microbiology and Cell Biology, Tokyo Metropolitan Institute of Medical Science, Setagaya-ku, Tokyo, Japan, **2** Division of Hepatology, Tokyo Metropolitan Komagome Hospital, Bunkyo-ku, Tokyo, Japan, **3** Transboundary Animal Diseases Center, Joint Faculty of Veterinary Medicine, Kagoshima University, Korimoto, Kagoshima, Japan, **4** Department of Virology II, National Institute of Infectious Diseases, Shinjuku-ku, Tokyo, Japan, **5** Laboratory of Immunobiology, Department of Pharmacy, School of Pharmacy, Hyogo University of Health Sciences, Chuo-ku, Kobe, Japan, **6** Laboratory of Immunodynamics, Department of Microbiology and Immunology, Osaka University Graduate School of Medicine, Suita, Osaka, Japan, **7** Chemo-Sero-Therapeutic Research Institute, Okubo, Kumamoto, Japan, **8** Department of Pathology, Tokyo Metropolitan Komagome Hospital, Bunkyo-ku, Tokyo, Japan, **9** Department of Molecular Preventive Medicine, School of Medicine, University of Tokyo, Bunkyo-ku, Tokyo, Japan

Abstract

Chronic hepatitis C, which is caused by infection with the hepatitis C virus (HCV), is a global health problem. Using a mouse model of hepatitis C, we examined the therapeutic effects of a recombinant vaccinia virus (rVV) that encodes an HCV protein. We generated immunocompetent mice that each expressed multiple HCV proteins via a Cre/*loxP* switching system and established several distinct attenuated rVV strains. The HCV core protein was expressed consistently in the liver after polyinosinic acid–polycytidylic acid injection, and these mice showed chronic hepatitis C-related pathological findings (hepatocyte abnormalities, accumulation of glycogen, steatosis), liver fibrosis, and hepatocellular carcinoma. Immunization with one rVV strain (rVV-N25), which encoded nonstructural HCV proteins, suppressed serum inflammatory cytokine levels and alleviated the symptoms of pathological chronic hepatitis C within 7 days after injection. Furthermore, HCV protein levels in liver tissue also decreased in a CD4 and CD8 T-cell-dependent manner. Consistent with these results, we showed that rVV-N25 immunization induced a robust CD8 T-cell immune response that was specific to the HCV nonstructural protein 2. We also demonstrated that the onset of chronic hepatitis in CN2-29$^{(+/-)}$/MxCre$^{(+/-)}$ mice was mainly attributable to inflammatory cytokines, (tumor necrosis factor) TNF-α and (interleukin) IL-6. Thus, our generated mice model should be useful for further investigation of the immunological processes associated with persistent expression of HCV proteins because these mice had not developed immune tolerance to the HCV antigen. In addition, we propose that rVV-N25 could be developed as an effective therapeutic vaccine.

Citation: Sekiguchi S, Kimura K, Chiyo T, Ohtsuki T, Tobita Y, et al. (2012) Immunization with a Recombinant Vaccinia Virus That Encodes Nonstructural Proteins of the Hepatitis C Virus Suppresses Viral Protein Levels in Mouse Liver. PLoS ONE 7(12): e51656. doi:10.1371/journal.pone.0051656

Editor: Naglaa H. Shoukry, University of Montreal, Canada

Received March 13, 2012; **Accepted** November 5, 2012; **Published** December 17, 2012

Funding: This study was supported by grants from the Ministry of Education, Culture, Sports, Science, and Technology of Japan; the Program for Promotion of Fundamental Studies in Health Sciences of the Pharmaceuticals and Medical Devices Agency of Japan; and the Ministry of Health, Labor, and Welfare of Japan. The funders had no role in study design, data collection and analysis, decision to publish, or preparation of the manuscript.

Competing Interests: The authors have declared that no competing interests exist.

* E-mail: kohara-mc@igakuken.or.jp

Introduction

Hepatitis C virus (HCV) is a major public health problem; approximately 170 million people are infected with HCV worldwide [1]. HCV causes persistent infections that can lead to chronic liver diseases such as chronic hepatitis, liver cirrhosis, and hepatocellular carcinoma (HCC) [2]. Antiviral drugs are not highly effective in individuals with a chronic infection; furthermore, an effective vaccine against HVC has not been developed. A convenient animal model of HCV infection will greatly facilitate the development of an effective HCV vaccine.

Transgenic mice that express HCV proteins have been generated to study HCV expression [3,4]; however, in each of these cases, the relevant transgenes is expressed during embryonic development; therefore, the transgenic mice become immunotolerant to the transgenic products, and consequently, the adult mice are not useful for investigations of the pathogenesis of chronic hepatitis C. To address this problem, we developed a system that can drive conditional expression of an HCV transgene; our system involves the Cre/*loxP* system and a recombinant adenovirus capable of expressing Cre recombinase [5,6]. Concerns have been expressed that an adenovirus and transient expression of HCV proteins could induce immune responses [5] and, therefore, obscure any evidence of the effect of the host immune responses on chronic liver pathology. Therefore, here, we used a Cre/*loxP* switching system to generate an immunocompetent mouse model

of HCV protein expression; with this system, we could study the host immune responses against HCV proteins.

Folgori et al. (2006) reported effective vaccination of chimpanzees with an adenoviral vector and plasmid DNA encoding the HCV nonstructural region. This technique protected the liver tissues from acute hepatitis, which results when whole animals are challenged with virus [7]. However, this vaccine has not yet been shown to be effective against chronic HCV infection.

Here, we aimed to address how HCV expression causes chronic liver diseases and to provide new options for HCV vaccine development. Using LC16m8, a highly attenuated strain of vaccinia virus (VV), we generated three recombinant vaccinia viruses (rVVs) that each encoded one of three different HCV proteins and found that one recombinant virus (rVV-N25), which encoded nonstructural HCV proteins, resolved pathological chronic hepatitis C symptoms in the liver. We also found that immunization with rVV-N25 suppressed HCV core protein levels in the livers of transgenic mice; moreover, this suppression was mediated by CD4 and CD8 T cells, as has been previously reported [8].

Results

Generation of a Model of Persistent HCV Protein Expression

To produce adult mice that express an HCV transgene, we bred CN2-29 transgenic mice, which carry an HCV transgene, [5,6,9] with Mx1-Cre transgenic mice [10], which express Cre recombinase in response to interferon (IFN)-α or a chemical inducer of IFN-α, poly(I:C) (Figure 1A). Following poly(I:C) injection, the HCV transgene was rearranged, and HCV sequences were expressed in the livers of F1 progeny (CN2-$29^{(+/-)}$/$MxCre^{(+/-)}$ mice) within 7 days after poly(I:C) injection (Figure 1B).

To evaluate the characteristic features of these CN2-$29^{(+/-)}$/$MxCre^{(+/-)}$ mice, we analyzed serum alanine aminotransferase (ALT) and liver HCV core protein levels after poly(I:C) injection. As illustrated in Figure 1C, serum ALT levels increased and reached a peak at 24 h after the first poly(I:C) injection; this elevation appeared to be a direct result of the poly(I:C) treatment, which causes liver injury [11]. After this peak, serum ALT levels dropped continuously until day 4, and then ALT levels began to increase, as did HCV core protein levels. Thereafter, the HCV core protein was expressed consistently for at least 600 days.

Histological analysis showed HCV core protein expression in most hepatocytes of the transgenic mice; these mice showed evidence of lymphocytic infiltration that was caused by the HCV core proteins (Figure 1D and E). These observations, in addition to the modified histology activity index (HAI) scores, indicated that expression of HCV proteins caused chronic hepatitis in the CN2-$29^{(+/-)}$/$MxCre^{(+/-)}$ mice because a weak, though persistent, immune response followed an initial bout of acute hepatitis (Figure S1). Moreover, we observed a number of other pathological changes in these mice – including swelling of hepatocytes, abnormal architecture of liver-cell cords, abnormal accumulation of glycogen, steatosis, fibrosis, and HCC (Figures 1E and F, Table S1). Steatosis was mild in the younger mice (day 21) and became increasingly severe over time (days 120 and 180; Figure S2). Importantly, none of the pathological changes were observed in the CN2-$29^{(+/-)}$/$MxCre^{(-/-)}$ mice after poly(I:C) injection (Figure 1F).

Recombinant Vaccinia Virus Immunization in HCV Transgenic Mice

To determine whether activation of the host immune response caused the reduction with HCV protein levels in the livers of CN2-$29^{(+/-)}$/$MxCre^{(+/-)}$ mice, we used a highly attenuated VV strain, LC16m8, to generate three rVVs [12]. Each rVV encoded a different HCV protein; rVV-CN2 encoded mainly structural proteins, rVV-N25 encoded nonstructural proteins, and rVV-CN5 encoded the entire HCV protein region (Figure 2A). Because rVVs can express a variety of proteins and induce strong and long-term immunity, they have been evaluated as potential prophylactic vaccines [13].

We used western blots to confirm that each HCV protein was expressed in cell lines. Each of seven proteins – the core, E1, E2, NS3-4A, NS4B, NS5A, and NS5B – was recognized and labeled by a separate cognate antibody directed (Figure S3). To induce effective immune responses against HCV proteins in transgenic mice, we injected an rVV-HCV (rVV-CN2, rVV-CN5, or rVV-N25) or LC16m8 (as the control) intradermally into CN2-$29^{(+/-)}$/$MxCre^{(+/-)}$ mice 90 days after poly(I:C) injection (Figure 2B). Analysis of liver sections 7 days after immunization with rVV-N25 revealed dramatic improvement in a variety of pathological findings associated with chronic hepatitis – including piecemeal necrosis, hepatocyte swelling, abnormal architecture of liver-cell cords, abnormal accumulation of glycogen, and steatosis (Figures 2C–E). Collectively, these results demonstrated that only the rVV-N25 treatment resulted in histological changes indicative of improvement in the chronic hepatitis suffered by the transgenic mice.

To determine whether rVV-N25 treatment induced the same effect in other strains of HCV transgenic mice, we analyzed RzCN5-$15^{(+/-)}$/$MxCre^{(+/-)}$ mice, which express all HCV proteins; in these mice, chronic hepatitis was resolved within 28 days of immunization with rVV-N25. Taken together, these findings indicated that rVV-N25 had a dramatic therapeutic effect on both types of HCV transgenic mice (Figure S4).

Treatment with rVV-N25 Reduced the HCV Core Protein Levels in the Livers

To assess in detail the effects of rVV-HCV immunization on HCV protein clearance from the livers of CN2-$29^{(+/-)}$/$MxCre^{(+/-)}$ mice, we monitored the levels of HCV core protein in liver samples via ELISA. We found that within 28 days after immunization the HCV core protein levels were significantly lower in livers of rVV-N25-treated mice than in those of control mice (Figure 3A). Immunohistochemical analysis indicated that, within 28 days after immunization, levels of HCV core protein were substantially lower in the livers of CN2-$29^{(+/-)}$/$MxCre^{(+/-)}$ mice than in those of control mice (Figure 3B). Importantly, neither resolution of chronic hepatitis nor reduction in the HCV protein levels was observed in the mice treated with LC16m8, rVV-CN2, or rVV-CN5. These results indicated that HCV nonstructural proteins might be important for effects of therapeutic vaccines. In contrast, rVV-CN5 which encoded HCV structural and non-structural proteins did not show any significant effects. These results indicated that HCV structural proteins might have inhibited the therapeutic effects of the non-structural proteins. Therefore, it may be important to exclude the HCV structural proteins (aa 1–541) as antigenic proteins when developing therapeutic vaccines against chronic hepatitis C.

In addition, we measured serum ALT levels in CN2-$29^{(+/-)}$/$MxCre^{(+/-)}$ mice from all four treatment groups 28 days after rVV-HCV immunization. Serum ALT levels were not significant-

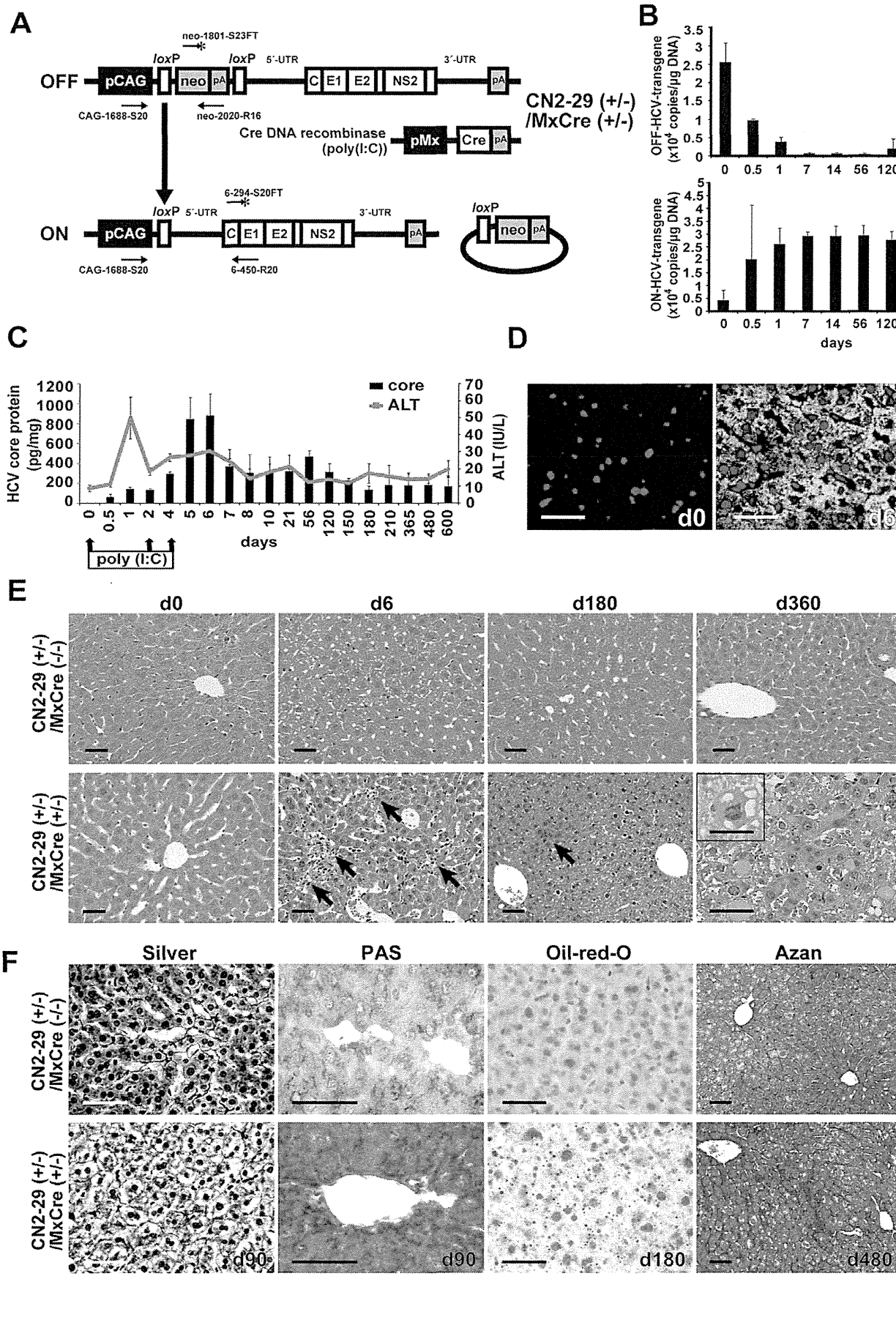
A
neo-1801-S23FT
loxP
loxP
5′-UTR
3′-UTR
OFF
pCAG
neo
pA
C
E1
E2
NS2
pA
CAG-1688-S20
neo-2020-R16
CN2-29 (+/-)
/MxCre (+/-)
Cre DNA recombinase
(poly(I:C))
pMx
Cre
pA
6-294-S20FT
loxP
5′-UTR
3′-UTR
ON
pCAG
C
E1
E2
NS2
pA
loxP
neo
pA
CAG-1688-S20
6-450-R20
B
OFF-HCV-transgene
(x10⁴ copies/μg DNA)
3.5
3
2.5
2
1.5
1
0.5
0
0
0.5
1
7
14
56
120
180
360
ON-HCV-transgene
(x10⁴ copies/μg DNA)
5
4.5
4
3.5
3
2.5
2
1.5
1
0.5
0
0
0.5
1
7
14
56
120
180
360
days
C
HCV core protein
(pg/mg)
1200
1000
800
600
400
200
0
core
ALT
ALT (IU/L)
70
60
50
40
30
20
10
0
0
0.5
1
2
4
5
6
7
8
10
21
56
120
150
180
210
365
480
600
days
poly (I:C)
D
d0
d6
E
d0
d6
d180
d360
CN2-29 (+/-)
/MxCre (-/-)
CN2-29 (+/-)
/MxCre (+/-)
F
Silver
PAS
Oil-red-O
Azan
CN2-29 (+/-)
/MxCre (-/-)
CN2-29 (+/-)
/MxCre (+/-)
d90
d90
d180
d480

Figure 1. Pathogenesis in immunocompetent mice with persistent HCV expression. (**A**) Structure of CN2-29$^{(+/-)}$/MxCre$^{(+/-)}$ and the Cre-mediated activation of the transgene unit. R6CN2 HCV cDNA was cloned downstream of the CAG promoter, neomycin-resistant gene (*neo*), and poly A (pA) signal flanked by two *loxP* sequences. This cDNA contains the core, E1, E2, and NS2 regions. (**B**) Cre-mediated genomic DNA recombination. After poly(I:C) injection, genomic DNA was extracted from liver tissues and analyzed by quantitative RTD-PCR for Cre-mediated transgenic recombination. The transgene was almost fully recombined in transgenic mouse livers 7 days after the injection. In all cases, n = 3 mice per group. (**C**) HCV core protein expression was sustained for at least 600 days after poly(I:C) injection. (**D**) Immunohistochemical analysis revealed that most hepatocytes expressed the HCV core protein within 6 days after injection. (**E**) Liver sections from CN2-29$^{(+/-)}$/MxCre$^{(+/-)}$ mice after the poly(I:C) injection. Infiltrating lymphocytes (arrows) were observed on days 6 and 180; Hepatocellular carcinoma (HCC) was observed on day 360. In contrast, these pathological changes were not observed in CN2-29$^{(+/-)}$/MxCre$^{(-/-)}$ mice after the injection. The inset image shows abnormal mitosis in a tumor cell. (**F**) Hepatocyte swelling and abnormal architecture of liver-cell cords (silver staining), as well as abnormal glycogen accumulation (PAS staining) were observed on day 90 in CN2-29$^{(+/-)}$/MxCre$^{(+/-)}$ mice. We observed steatosis (oil-red-O staining) on day 180 and, subsequently, fibrosis (Azan staining) on day 480. The scale bars indicate 50 μm.
doi:10.1371/journal.pone.0051656.g001

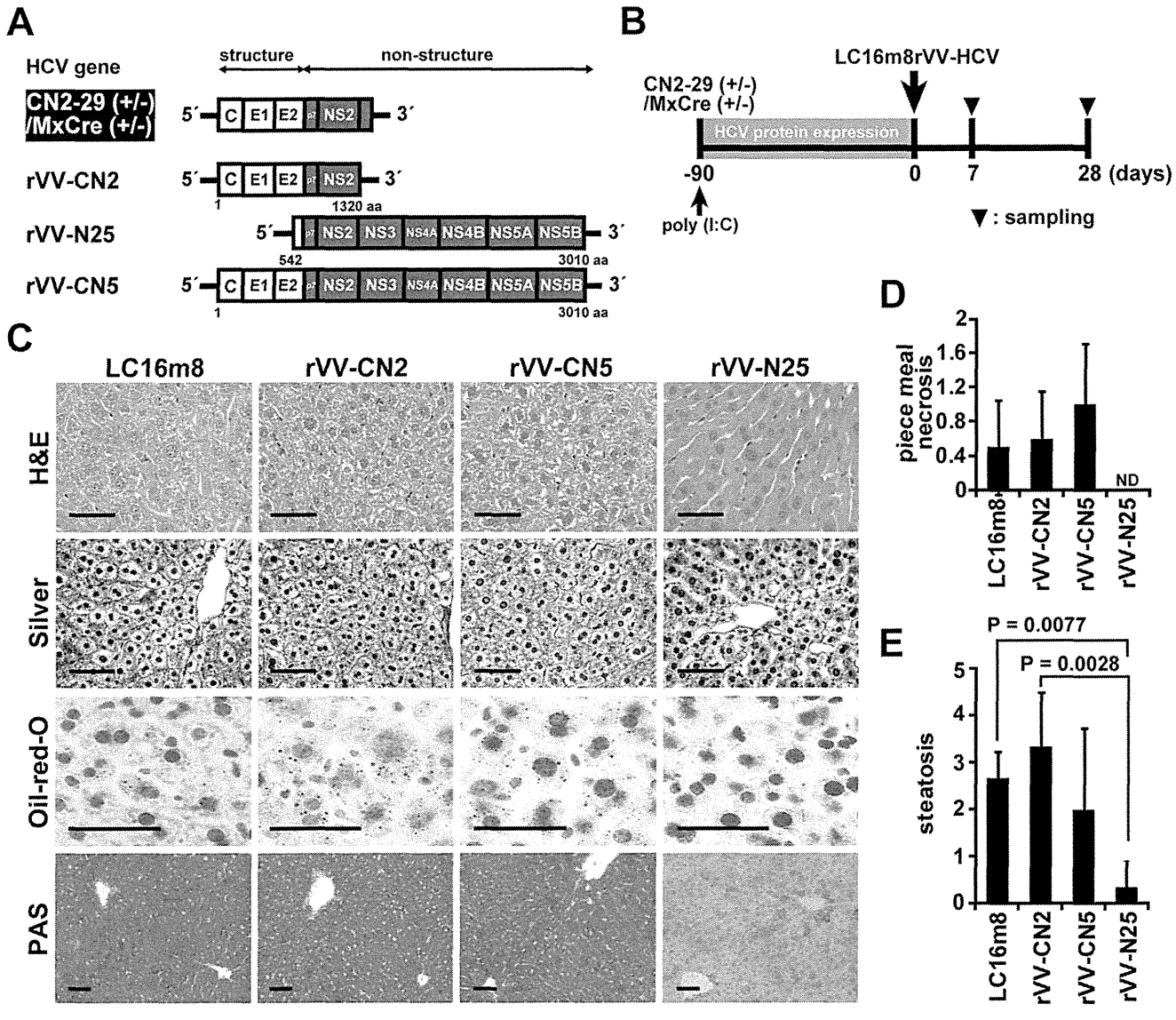

Figure 2. Effects of rVV-HCV treatment on the CN2-29$^{(+/-)}$/MxCre$^{(+/-)}$ mice. (**A**) HCV gene structure in the CN2-29$^{(+/-)}$/MxCre$^{(+/-)}$ mice and recombinant vaccinia viruses (rVV-HCV). MxCre/CN2-29 cDNA contains the core, E1, E2, and NS2 regions. The rVV-CN2 cDNA contains the core, E1, E2, and NS2 regions. The rVV-N25 cDNA contains the NS2, NS3, NS4A, NS4B, NS5A, and NS5B regions. The rVV-CN5 cDNA contains the entire HCV region. (**B**) Four groups of CN2-29$^{(+/-)}$/MxCre$^{(+/-)}$ mice were inoculated intradermally with rVV-CN2, rVV-N25, rVV-CN5, or LC16m8 90 days after the poly(I:C) injection. Blood, liver, and spleen tissue samples were collected 7 and 28 days after the inoculation. (**C**) Liver sections from the four groups of CN2-29$^{(+/-)}$/MxCre$^{(+/-)}$ mice 7 days after the inoculation. The sections were stained with H&E, silver, oil-red-O, or PAS. The scale bars indicate 50 μm. (**D**) Histological evaluation of piecemeal necrosis in the four groups of CN2-29$^{(+/-)}$/MxCre$^{(+/-)}$ mice 7 days after inoculation. (**E**) Histological evaluation of steatosis in the four groups of CN2-29$^{(+/-)}$/MxCre$^{(+/-)}$ mice 7 days after inoculation. Significant relationships are indicated by a P-value.
doi:10.1371/journal.pone.0051656.g002

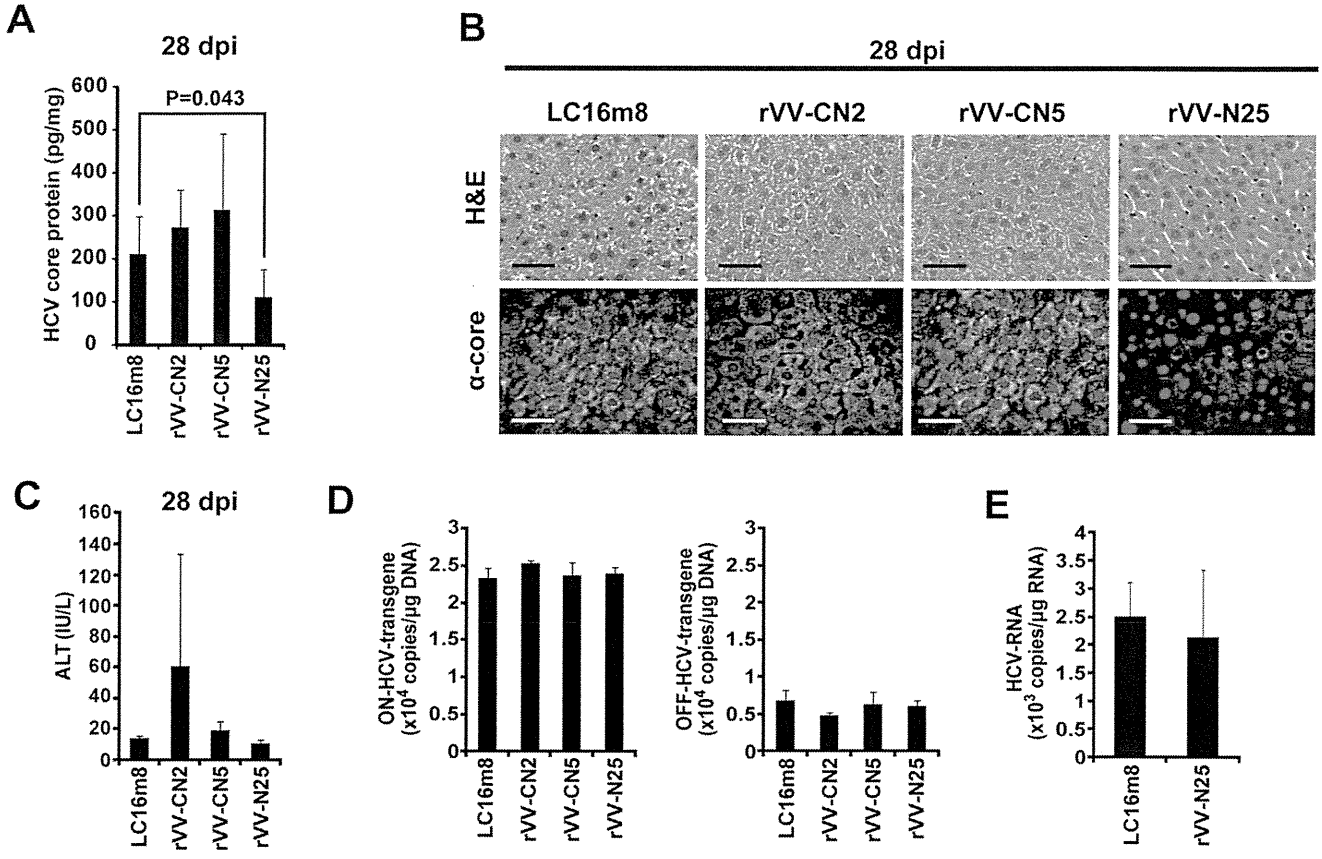

Figure 3. Effects of HCV core protein expression on the livers of CN2-29$^{(+/-)}$/MxCre$^{(+/-)}$ mice inoculated with rVV-HCV. (**A**) Expression of the HCV core protein in the four treatment groups of CN2-29$^{(+/-)}$/MxCre$^{(+/-)}$ mice 28 days after the inoculation. Significant relationships are indicated by a P-value. (**B**) H&E staining and immunohistochemical analysis for HCV core protein in the LC16m8-, rVV-CN2-, rVV-CN5-, or rVV-N25-treated CN2-29$^{(+/-)}$/MxCre$^{(+/-)}$ mice 28 days after the inoculation. Liver sections were stained with the anti-core monoclonal antibody. The scale bars indicate 50 μm. (**C**) Effects of HCV core protein expression on serum ALT levels in the four treatment groups of CN2-29$^{(+/-)}$/MxCre$^{(+/-)}$ mice 28 days after immunization. (**D**) Cre-mediated genomic DNA recombination in the four treatment groups 28 days after immunization. (**E**) Expression of HCV mRNA in the LC16m8- or rVV-N25-treated CN2-29$^{(+/-)}$/MxCre$^{(+/-)}$ mice 28 days after immunization. In all cases, n = 6 mice per group.
doi:10.1371/journal.pone.0051656.g003

ly different in the rVV-N25-treated mice and control mice (Figure 3C); this finding indicated that rVV-N25 treatment did not cause liver injury and that the antiviral effect was independent of hepatocyte destruction.

We hypothesized that the reduction in the levels of HCV core protein in rVV-HCV-treated mice was not caused by cytolytic elimination of hepatocytes that expressed HCV proteins. To investigate this hypothesis, we conducted an RTD-PCR analysis of genomic DNA from liver samples of CN2-29$^{(+/-)}$/MxCre$^{(+/-)}$ mice. The recombined transgene was similar in rVV-N25-treated and control mice 28 days after immunization (Figure 3D). We also measured the expression of HCV mRNA in LC16m8-treated CN2-29$^{(+/-)}$/MxCre$^{(+/-)}$ mice with that in rVV-N25-treated CN2-29$^{(+/-)}$/MxCre$^{(+/-)}$ mice 28 days after immunization; the HCV mRNA levels did not differ between rVV-N25-treated CN2-29$^{(+/-)}$/MxCre$^{(+/-)}$ and control mice (Figure 3E). These results indicated that rVV-N25-induced suppression of HCV core protein expression could be controlled at a posttranscriptional level.

Role of CD4 and CD8 T cells in rVV-N25-treated Mice

Viral clearance is usually associated with CD4 and CD8 T-cell activity that is regulated by cytolytic or noncytolytic antiviral mechanism [14]. To determine whether CD4 or CD8 T-cell activity was required for the reduction in HCV core protein levels in the livers of transgenic mice, we analyzed the core protein levels in CN2-29$^{(+/-)}$/MxCre$^{(+/-)}$ mice immunized with rVV-N25 in the absence of CD4 or CD8 T cells (Figure 4A). As expected, the mice lacking CD4 or CD8 T cells failed to show a reduction in HCV core protein levels (Figure 4B).

However, in mice lacking either CD4 or CD8 T-cells, the pathological changes associated with chronic hepatitis were resolved following rVV-N25 immunization, and the steatosis score of rVV-N25-treated mice was significantly lower than that of control mice (Figures 4C–E). These results indicated that CD4 and CD8 T cells were not responsible for the rVV-N25-induced amelioration of histological findings and that other inflammatory cell types may play an as-yet-unidentified role in the resolution of the pathological changes in these mice.

rVV-N25 Immunization Induced an NS2-specific Activated CD8 T cells Response

Because we found that HCV protein reduction in the liver required CD8 T cells, we tested whether HCV-specific CD8 T cells were present in splenocytes 28 days after immunization. To determine the functional reactivity of HCV-specific CD8$^+$ T cells, we performed a CD107a mobilization assay and intracellular IFN-γ staining. CN2-29 transgenic mice expressed the HCV structural protein and the NS2 region. However, rVV-N25 comprised only